Train on Pins and Test on Obstacles for Rectilinear Steiner Minimum Tree

Xingbo Du, Ruizhe Zhong, Junchi Yan[*]
School of Computer Science & School of Artificial Intelligence, Shanghai Jiao Tong University
{duxingbo,zerzerzerz271828,yanjunchi}@sjtu.edu.cn

Abstract

Rectilinear Steiner Minimum Tree (RSMT) is widely used in Very Large Scale Integration (VLSI) and aims at connecting a set of pins using rectilinear edges while minimizing wirelength. Recently, learning-based methods have been explored to tackle this problem effectively. However, existing methods either suffer from excessive exploration of the search space or rely on heuristic combinations that compromise effectiveness and efficiency, and this limitation becomes notably exacerbated when extended to the obstacle-avoiding RSMT (OARSMT). To address this, we propose OAREST, a reinforcement learning-based framework for constructing an Obstacle-Avoiding Rectilinear Edge Sequence (RES) Tree. We theoretically establish the optimality of RES in obstacle-avoiding scenarios, which forms the foundation of our approach. Leveraging this theoretical insight, we introduce a dynamic masking strategy that supports parallel training across varying numbers of pins and extends to obstacles during inference. Empirical evaluations on both synthetic and real-world benchmarks show superior effectiveness and efficiency for RSMT and OARSMT problems, particularly in handling obstacles without training on them. Code available: https://github.com/Thinklab-SJTU/EDA-AI/.

1 Introduction

Rectilinear Steiner Minimum Tree (RSMT) and its obstacle-avoiding version named OARSMT are critical combinatorial problems in electronic design automation (EDA) in Very Large Scale Integration (VLSI) design [1, 2, 3]. As an NP-complete problem [4], the goal of RSMT is to connect a given set of pins using rectilinear edges, i.e., edges that are parallel to the axes, while minimizing the total wirelength. Recently, the RSMT problem [5, 6, 7, 8, 9], as well as the entire EDA community [10, 11, 12, 13], has received extensive attention from the machine learning (ML) community. However, with the increasing number of nets in modern technologies and particularly the incorporation of obstacles, existing ML-based methods suffer from various challenges.

We summarize the critical **challenges** for ML-based approaches in both vanilla RSMT and OARSMT problems in Table 1, including: 1) *Lack of efficient and accurate representations*: Efficient representations are essential for reducing the searching space (e.g., the action space in the reinforcement learning (RL) agent), which can otherwise become excessively complex and computationally exhaustive. Accurate representations, on the other hand, enable ML approaches to learn the global optimum in an end-to-end manner without relying on post-processing [7, 9] or integrating heuristics [8]. 2) *Multi-degree GPU parallelization*: Existing ML-based techniques [5, 6] typically require inputs of the same size, limiting their ability to handle multi-degree instances (i.e., instances with varying numbers of pins) in parallel. 3) *Obstacle avoidance*: The introduction of obstacles significantly increases problem complexity and further exacerbates the above two challenges.

[*]Correspondence to: Junchi Yan. This work was partly supported by NSFC (92370201).

Table 1: Comparisons of ML-based methods.

Method	Representation	End-to-End	Multi-Degree GPU-Parallelization	Obstacle Avoidance
REST [5]	RES (Optimal)	✓	✗	✗
EPST [6]	EPS	✓	✗	✗
Chen et al. [7]	Steiner Points	✗	✓	✓
Lin et al. [8]	OASG + SPF	✗	✓	✓
Chen et al. [9]	Steiner Points	✗	✓	✓
OAREST (ours)	RES (Optimal)	✓	✓	✓

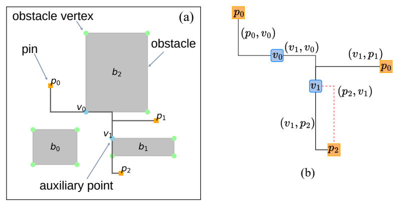

Figure 1: a) Different components. b) Rectilinear edges in an OARSMT.

To address these challenges, we first extend the rectilinear edge sequence (RES) representation, originally proposed in REST [5], to the OARSMT problem. Such an extension is nontrivial as the problem's structure is fundamentally altered. We theoretically demonstrate that RES can achieve optimality for both RSMT and OARSMT problems.

Building upon these theoretical insights, we propose a novel RL-based framework OAREST (Obstacle-Avoiding Rectilinear Edge Sequence Tree), designed to tackle multi-degree GPU parallelization and dynamic obstacle avoidance simultaneously. Within this framework, we introduce a dynamic masking strategy that selectively activates candidate corner vertices of obstacles, ensuring efficient and obstacle-aware decision-making. Empirical results on both synthetic and industrial benchmarks validate the effectiveness and efficiency of OAREST in solving RSMT and OARSMT problems. Particularly, the obstacles can be avoided effectively in OARSMT problems without training on any obstacles. **The main contributions are listed as follows:**

1) **Theoretical findings and derived RL framework**: We prove the optimality of the rectilinear edge sequence (RES) representation for the obstacle-avoiding rectilinear Steiner minimum tree (OARSMT) problem. Inspired by this, we introduce OAREST, an end-to-end RL framework based on the RES, which combines theoretical optimality with computational efficiency. To the best of our knowledge, OAREST is the first ML-based approach handling obstacles without training on obstacles.

2) **Novel dynamic masking strategy**: Within the RL framework, we devise a novel dynamic masking strategy that can not only handle multi-degree parallel training/inference on GPUs but also dynamically activate candidate obstacle vertices for effective obstacle avoidance. Thus, the OARSMT problems can be handled without training on any obstacles.

3) **Empirical advancements and efficient obstacle handling**: We perform experiments on extensive instances with/without obstacles and demonstrate comparable performance to advanced baselines. The results particularly highlight OAREST's robust capabilities in managing parallel inference and avoiding obstacles efficiently.

2 Preliminaries and Main Theorem

Before introducing the RL framework, we first propose key definitions in Sec. 2.1 and state the OARSMT problems in Sec. 2.2, based on which we introduce the main theorem in Sec. 2.3 that demonstrates the optimality of rectilinear edge sequence (RES) in OARSMT problems.

2.1 Definition

We introduce various definitions in OARSMT problems and visualize components in Fig. 1(a).

Definition 2.1. [Rectilinear Steiner Tree, RST] Given a finite set of pins[2] $\mathcal{P} = \{p_0, p_1, \cdots, p_{n-1}\}$ with each pin p_i having fixed coordinates (x_i, y_i), a rectilinear Steiner tree (RST) is a tree that connects all pins and some non-pin auxiliary points, where each edge is parallel to the coordinate axis. The non-pin auxiliary points are named **Steiner points**, which are used to minimize the total length.

Here, each edge is either horizontal or vertical. In OARSMT problems, RSTs are required to avoid overlapping with rectangular obstacles, which are defined as:

[2]We use 'pin' to distinguish from 'obstacle vertex' and 'Steiner points', and collectively name them 'points'.

Definition 2.2. [Rectangular Obstacles] Define $\mathcal{O} = \{o_0, o_1, \cdots, o_{m-1}\}$ as a group of rectangular regions. Each obstacle $o_i = (v_i^{(ld)}, v_i^{(lu)}, v_i^{(ru)}, v_i^{(rd)})$ is composed of four vertices in its left-down (ld), left-up (lu), right-up (ru), and right-down (rd) corners. Denote these vertices as $\mathcal{V}(\mathcal{O})$.

Note that any complex rectilinear obstacle (e.g., rectilinear polygons) can be easily achieved by combining different rectangular obstacles. To formulate RSTs in an OARSMT problem, we apply the rectilinear edge sequence (RES) [5] representation to our framework, defined as:

Definition 2.3. [Rectilinear Edge Sequence, RES] For a given set of pins $\mathcal{P} = \{p_0, p_1, \cdots, p_{n-1}\}$, its RES is a sequence with $n-1$ rectilinear edge pairs $((v_0, h_0), (v_1, h_1), \cdots, (v_{n-2}, h_{n-2}))$, where $v_i, h_i \in \{0, 1, \cdots, n-2\}$ denotes the indices of pins.

Note that rectilinear edges are non-commutative in rectilinear geometry, i.e., $(v, h) \neq (h, v)$. Specifically, (v, h) denotes a path where the vertical edge starts at v followed by a horizontal edge ending at h. A visualized example of rectilinear edges is shown in Fig. 1(b), where (p_2, v_1) and (v_1, p_2) are two distinct rectilinear edges. To keep RES always valid in RSMT construction problem, RES is required to satisfy: 1) $v_0 \neq h_0$; 2) For each rectilinear edge pair (v_i, h_i), exactly one of v_i, h_i is visited before by previous rectilinear edge pair, and the other is not. Details given by [5] is moved to Lemma A.4 in Appendix A. Other definitions that are only related to the proof of our main theory, including Hanan Grid and extended Hanan Grid, can be found in Appendix A.1.

2.2 Problem Statement

Based on the definitions, we formulate OARSMT as:

Definition 2.4. [Obstacle-Avoiding Rectilinear Steiner Tree, OARSMT] Given a finite set of pins $\mathcal{P} = \{p_0, p_1, \cdots, p_{n-1}\}$ and a set of rectangular obstacles $\mathcal{O} = \{o_0, o_1, \cdots, o_{m-1}\}$, an obstacle-avoiding rectilinear Steiner tree (OARSMT) is defined as:

$$T^* = \underset{T \in \mathcal{T}}{\text{argmin}} \sum_{e \in \mathcal{E}(T)} |e|, \tag{1}$$

under constraints: 1) T is a tree connecting all pins in $\mathcal{P}$, 2) $\forall e \in \mathcal{E}(T)$: e is parallel to coordinate axes, 3) $\forall e \in \mathcal{E}(T), \forall o_i \in \mathcal{O} : e \cap \text{int}(o_i) = \emptyset$, 4) $\mathcal{V}(T) \setminus \mathcal{P}$ are Steiner points. Here, $\mathcal{T}$ is the set of all rectilinear Steiner trees in terms of $\mathcal{P}$ and $\mathcal{O}$. Additionally, $|e|$ denotes the Manhattan length of edge e, $\mathcal{E}(T)$ represents the set of edges in tree T, $\mathcal{V}(T)$ is the set of vertices in T, and $\text{int}(o_i)$ denotes the interior region of obstacle o_i.

Intuitively, OARSMT aims to obtain a rectilinear tree with minimum length that avoids obstacles.

2.3 Main Theorem

Theorem 2.5. ***[Optimality of RES in OARSMT]*** *For any set of pins $\mathcal{P} = \{p_0, p_1, \cdots, p_{n-1}\}$ and a set of rectangular obstacles $\mathcal{O} = \{o_0, o_1, \cdots, o_{m-1}\}$, an optimal RES of $\mathcal{P} \cup \mathcal{V}'(\mathcal{O})$ can always be found such that its corresponding tree is an optimal OARSMT for $\mathcal{P}$ under obstacles $\mathcal{O}$. Here, $\mathcal{V}'(\mathcal{O}) \subset \mathcal{V}(\mathcal{O})$ is a subset of the corner vertices of all obstacles.*

This theorem demonstrates that an optimal RES can always be found to construct an optimal OARSMT. The proof can be found in Appendix A.3. Note that Theorem 2.5 gives us an insightful **intuition**: *In order to construct an OARSMT, we are only required to construct a RES that connects all pins and a subset of corner vertices of obstacles.*

3 Obstacle-Avoiding Rectilinear Edge Sequence Tree

Overview. We propose an RL-based framework to handle OARSMT. The overall pipeline is given in Fig. 2, while the connecting process of the rectilinear edge sequence (RES) is shown by a simple toy example in Fig. 2(d). Following [5], we use actor-critic networks to generate rectilinear edge sequence (RES) in Sec. 3.1. To accommodate multi-degree parallelization and obstacle handling, we introduce a novel dynamic masking strategy in Sec. 3.2. In Sec. 3.3, we provide a detailed discussion on our focus on multiple small instances in OARSMT problems and analyze the time complexity of the proposed framework.

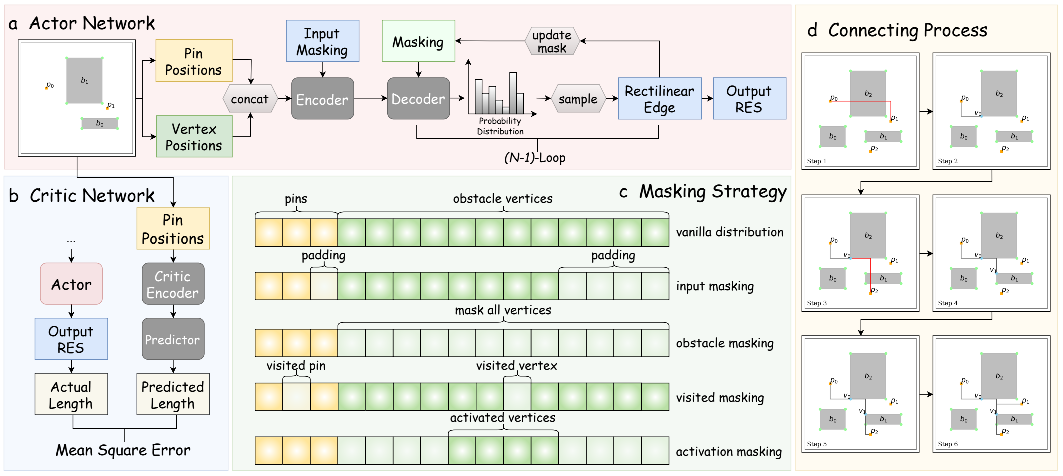

Figure 2: Pipeline of OAREST. a) Actor network that generates the rectilinear edge sequence (RES) step-by-step with dynamic masking strategies. b) Critic network that fits the actual length of RES. c) Dynamic masking strategies, including input masking, obstacle masking, visited masking, and activation masking, that enable the RES generation with multi-degree forward passing and obstacle avoidance. d) Visualization of the connecting process of OAREST on a toy sample with 3 pins (p_0, p_1, p_2) and 3 obstacles (b_0, b_1, b_2).

3.1 Generate RES using Actor-Critic Network

Similar to the objectives of REST [5], we utilize an actor-critic network to learn the construction of the rectilinear edge sequence (RES). Given the positions of all pins $\mathcal{P} = \{p_0, p_1, \cdots, p_{n-1}\}$, the actor network $\text{Actor}(r|\mathcal{P};\xi)$ with parameters ξ, as shown in Fig. 2(a), takes a series of sequential actions to generate the elements of the RES $r \in \mathcal{R}(\mathcal{P})$ and yields the probability of generating r, where $\mathcal{R}(\mathcal{P})$ is the set of all possible RES for $\mathcal{P}$. The actor network here is trained to generate the optimal RES. The critic network $\text{Critic}(\mathcal{P};\zeta)$ with parameters ζ, as depicted in Fig. 2(b), predicts the length of the RSMT of $\mathcal{P}$, which is trained to approximate its actual length $L(\mathcal{P}, r)$. Note that $L(\mathcal{P}, r)$ is actually the evaluation of the RES, which can be achieved linearly [5] and is assumed to approximate the actual RSMT length accurately.

More specifically, for each given pin set $\mathcal{P}$, the objective of the actor network is to minimize the expected advantage of the RSMT generated by $\text{Actor}(r|\mathcal{P};\xi)$, and we use the policy gradient algorithm REINFORCE [14] to compute the gradient:

$$\min_\xi \;\; \mathbb{E}_{r\sim R(\mathcal{P})} \left(\text{Critic}(\mathcal{P};\zeta) - L(\mathcal{P}, r)\right) \text{Actor}(r|\mathcal{P};\xi). \tag{2}$$

Conversely, the critic network's objective is to minimize the mean square error (MSE) between its predicted length and the actual length of RSMT:

$$\min_\zeta \;\; \mathbb{E}_{r\sim R(\mathcal{P})} \|\text{Critic}(\mathcal{P};\zeta) - L(\mathcal{P}, r)\|_2^2. \tag{3}$$

In practice, given a batch of pin sets $\{\mathcal{P}_0, \mathcal{P}_1, \cdots, \mathcal{P}_{b-1}\}$, one RES r_i is generated for each $\mathcal{P}_i (i \in \{0, \cdots, b-1\})$. Consequently, Eq. 2 and Eq. 3 can be reformulated as:

$$\begin{aligned} &\min_\xi \frac{1}{b} \sum_{i=1}^{b} \left(\text{Critic}(\mathcal{P}_i;\zeta) - L(\mathcal{P}_i, r_i)\right) \text{Actor}(r_i|\mathcal{P}_i;\xi), \\ &\min_\zeta \frac{1}{b} \sum_{i=1}^{b} \|\text{Critic}(\mathcal{P}_i;\zeta) - L(\mathcal{P}_i, r_i)\|_2^2. \end{aligned} \tag{4}$$

These objectives are optimized simultaneously. In inference, only $\text{Actor}(r_i|\mathcal{P}_i;\xi)$ is required to generate the RES r_i with the highest probability. Note that both training and inference are end-to-end.

3.2 Dynamic Masking

The key issues in Sec. 3.1 are twofold: 1) the actor-critic network requires inputs and outputs of fixed sizes to enable GPU parallelization, and 2) obstacle constraints are not incorporated. To address these issues, as illustrated in Fig. 2(c), we propose a dynamic masking mechanism, which dynamically adjusts valid action spaces during each decision step, enabling efficient handling of variable input sizes and the integration of obstacle constraints.

First, we use a tensor $\mathbf{I} \in \mathbb{R}^{b\times(\hat{n}+4\hat{m})\times 2}$ to represent the input of the actor net, where b is the batch size, $\hat{n}$ is the max number of pins of the pin set in a batch $\{\mathcal{P}_i\}_{i=0}^{n-1}$, and $\hat{m}$ is the max number of obstacles in $\{\mathcal{O}_i\}_{i=0}^{m-1}$. The value '4' here means the four corner vertices of an obstacle, and '2' means the x- and y-axis of coordinates. For the instances with $n(<\hat{n})$ pins or $m(<\hat{m})$ obstacles, we pad the corresponding elements to -1 in the input tensor. The dynamic mechanism is then devised with the following components:

Input/Obstacle Masking. The input mask is devised to ignore the computations for invalid elements. It is constructed using a matrix $\mathbf{M}^{\text{input}} \in \{0,1\}^{b\times(\hat{n}+4\hat{m})}$. The obstacle mask ensures that the actor network does not select an obstacle vertex as the first element of the RES, which is constructed using a matrix $\mathbf{M}^{\text{ob}} \in \{0,1\}^{b\times(\hat{n}+4\hat{m})}$. Each element of $\mathbf{M}^{\text{input}}$ and $\mathbf{M}^{\text{ob}}$ is defined as:

$$\mathbf{M}^{\text{input}}_{i,j} = \begin{cases} 0, & \text{if } \mathbf{I}_{i,j,0} = \mathbf{I}_{i,j,1} = -1, \\ 1, & \text{otherwise,} \end{cases} \qquad \mathbf{M}^{\text{ob}}_{i,j} = \begin{cases} 0, & \text{if } j > \hat{n}, \\ 1, & \text{otherwise.} \end{cases} \tag{5}$$

Visited/Activation Masking. Based on the properties of the RES (as described in Sec. 2.1), each rectilinear edge must have exactly one visited and one unvisited element. The visited mask enforces this condition. It is represented by a matrix $\mathbf{M}^{\text{visited}} \in \{0,1\}^{b\times(\hat{n}+4\hat{m})}$. On the other hand, the activation masking activates parts of the obstacle vertices and is used to avoid obstacles when generating the RES, which is initialized as $\mathbf{M}^{\text{act}} = \mathbf{M}^{\text{ob}}$. Each time a newly generated rectilinear edge overlaps with one or more obstacles, the elements in $\mathbf{M}^{\text{act}}$ corresponding to the corner vertices of these obstacles are activated. Each element of $\mathbf{M}^{\text{visited}}$ and $\mathbf{M}^{\text{act}}$ is defined as:

$$\mathbf{M}^{\text{visited}}_{i,j} = \begin{cases} 0, & \text{if } j \text{ is an element in RES } r_i, \\ 1, & \text{otherwise.} \end{cases} \qquad \mathbf{M}^{\text{act}}_{i,j} = \begin{cases} 0, & \text{if } j \text{ is inactivated,} \\ 1, & \text{otherwise.} \end{cases} \tag{6}$$

When a newly generated rectilinear edge does not overlap with obstacles, the mask is re-initialized as $\mathbf{M}^{\text{act}} = \mathbf{M}^{\text{ob}}$. In practice, the actor net sequentially determines which pin or vertex to generate. Each action is based on a probability distribution matrix $\mathbf{S} \in \mathbb{R}^{b\times(\hat{n}+4\hat{m})}$. The combination of dynamic masks is then used to select the elements in RES:

- To begin with, we sample a batch of *start* points from $\mathbf{S}^{\text{start}} = \mathbf{S} \circ \left(\mathbf{M}^{\text{input}} \wedge \mathbf{M}^{\text{ob}}\right)$, where $\circ$ is the Hadamard product (element-wise multiplication) and $\wedge$ represents logical 'AND', which evaluates to true only when both operands are true. This ensures that only valid pins are selected as the first element of a RES.
- For a batch of rectilinear edges, we select a batch of *visited* points from $\mathbf{S}^{\text{visited}} = \mathbf{S} \circ \left(\mathbf{1} - \mathbf{M}^{\text{visited}}\right)$. For the same batch of rectilinear edges, we select a batch of *unvisited* points from $\mathbf{S}^{\text{unvisited}} = \mathbf{S} \circ \left(\mathbf{M}^{\text{input}} \wedge \mathbf{M}^{\text{visited}} \wedge \mathbf{M}^{\text{act}}\right)$. This implies that the selected points must be valid unvisited ones while $\mathbf{M}^{\text{act}}$ ensures that the rectilinear edge does not overlap with any obstacles, as governed by Eq. 6.

Equipped with the dynamic masking strategy, OAREST is capable of addressing the multi-degree training and inference for RSMT problems, and can infer directly on OARSMT problems without training with any obstacle. Functions and executions of different masks are summarized in Table 2.

3.3 Remarks

Intuition on generalization to obstacles and strategy. Theorem 2.5 suggests that it suffices to construct a RES that connects all pins and a subset of obstacle corner vertices. The RL agent's goal is then to connect these pins and selected corners. Since OAREST is trained only on pins but must also connect corner vertices, a natural idea is to treat corner vertices as pins. However, this raises

Table 2: Functions and executions of different masks.

Masking	Function	Execution
Input	Achieve multi-degree GPU parallelization.	Mask invalid elements at the beginning.
Obstacle	1) Avoid choosing a corner vertex as the first element of the RES; 2) Avoid unnecessary corner vertex connection.	1) Mask all obstacle vertices at the beginning. 2) When a newly generated rectilinear edge does not overlap with obstacles, re-initialize the activation mask as the obstacle mask.
Visited	Construct valid RES following the criterion of Lemma A.4.	Use masking to generate a visited point and an unvisited point for each rectilinear edge.
Activation	Avoid generating rectilinear edges that overlap with obstacles.	Each time a newly generated rectilinear edge overlaps with one or more obstacles, the elements in the activation masking corresponding to the corner vertices of these obstacles are activated.

two issues: (1) not all corner vertices need to be connected, and (2) the resulting edges may overlap obstacles. Accordingly, obstacle masking is used to avoid unnecessary corner-vertex connections (issue 1), and an activation mask is used to prevent overlap with obstacles (issue 2). Notably, both masking strategies can be applied purely at inference.

Time Complexity for Inference. The overall time complexity for inference is $O\left((\hat{n}+\hat{m}) \cdot T_{\text{batch}}/b\right)$, where T_{batch} represents the inference time for a single batch, and b denotes the batch size. This complexity arises because all computations within the actor network are linear with respect to $\hat{n}+\hat{m}$. The high efficiency of the framework can thus be attributed to the ability to handle large batch sizes, particularly for multiple small-sized instances.

Single Large Instance vs. Multiple Small Instances. Lots of previous works [7, 8, 9] primarily focus on constructing OARSMTs of large-scale instances with hundreds or even thousands of pins; however, these approaches often rely on heuristic tools, which limit their performance in GPU parallelization. In contrast, this paper takes an orthogonal approach by focusing on OARSMT construction for multiple small instances, achieving significant improvements in parallel efficiency. Furthermore, its focus on small-scale instance construction makes it more aligned with practical scenarios in certain industrial applications. As shown in Table 3, we analyze benchmarks from the ICCAD19 [15] global routing contest, a highly regarded industry competition. The results reveal that most nets contain fewer than 10 pins. Specifically, the proportion of nets with more than 100 pins is only 0.002%, highlighting the importance of efficient inference for multiple small instances.

4 Experiments

Experiments were conducted on a machine equipped with an AMD EPYC 7402 24-Core Processor, an NV GeForce RTX 4090, and 512 GB of RAM. To ensure robust evaluations, experiments were repeated using three distinct seeds. The experimental protocols are detailed in Section 4.1, while the main results for RSMT/OARSMT are presented in Sections 4.2/4.3. In Sec. 4.4, we perform ablation studies, show generality on untrained degrees, and evaluate the performance on real-world circuits.

4.1 Experimental Protocols

Datasets. We evaluated the proposed method using two datasets. The first consists of randomly generated test data as described by REST [5]. This dataset includes varying degrees ranging from 5 to 50 in increments of 5, referred to as R5, R10, etc. Each subset contains 10 k test instances. To assess the method's capability in handling obstacles, we further introduced 5 and 10 random obstacles to the test cases in R5, R10, etc. The second dataset consists of real-world global routing benchmarks from ICCAD19 [15], which is directly evaluated using the model trained on R5–R50.

Metrics. We employ the total wirelength as the primary metric for RSMT and OARSMT, which is calculated using the total Manhattan distance of a tree:

$$L = \sum_{e\in\mathcal{E}} \text{length}(e) = \sum_{(v_i,v_j)\in\mathcal{E}} \left(|x_i - x_j| + |y_i - y_j|\right), \tag{7}$$

Table 3: Statistics of nets $(\times 10^3)$ with different numbers of pins in ICCAD19 [15] benchmark.

# Pins	ispd18_test{1-10}		ispd19_test{1-10}	
	# Nets $(\times 10^3)$	proportion (%)	# Nets $(\times 10^3)$	proportion (%)
<3	579	57.07	1,791	57.17
3-10	387	38.12	1,197	38.21
11-20	13	1.29	40	1.28
21-30	4	0.42	13	0.41
31-40	16	1.58	47	1.49
41-50	4	0.44	13	0.42
51-100	11	1.08	32	1.02
>100	0.02	0.002	0.06	0.002

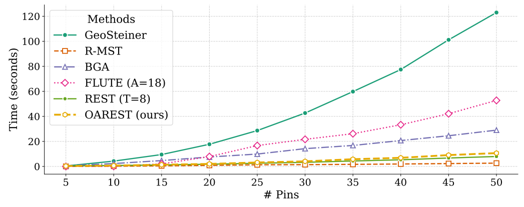

Figure 3: Runtime (seconds) of RSMT methods for testing $10\,\mathrm{k}$ instances on varied pins.

where $\mathcal{E}$ is the edge set of the tree. The average percentage error $(L - L_{\text{opt}})/L_{\text{opt}}$ is then utilized to measure the gap from the optimal solution L_{opt} obtained by the exact algorithm GeoSteiner [16]. For OARSMT problems, we further employ the overlap metric:

$$\text{overlap}(e, o_k) = \begin{cases} 1, & \text{if } e \cap \text{int}(o_k) \neq \emptyset, \\ 0, & \text{Otherwise}, \end{cases}, \qquad O = \sum_{e \in \mathcal{E}} \sum_{k=1}^{n} \text{overlap}(e, o_k), \tag{8}$$

where $\text{int}(o_k)$ is the interior region of obstacle $o_k \in \mathcal{O}$.

Baselines. RSMT baselines include GeoSteiner [16], R-MST [17], BGA [18], FLUTE [19], and REST [5]. For OARSMT, we evaluate wirelength, overlaps, and runtime against GeoSteiner [16], OARST [20], and OARSMT [21], respectively. Details are shown in Appendix B.2.

Other Settings and Results. We show other experimental settings, including the model structures of the actor-critic networks, hyperparameters, training/inference strategies, and more visualizations in Appendix B.3 - B.6.

4.2 Main Results of RSMT

Table 4 shows the average percentage error of algorithms compared to the exact algorithm GeoSteiner [16] across various scales of random instances. R-MST [17] has a substantial gap from the optimal GeoSteiner. Other approaches, including BGA [18], FLUTE [19], and REST [5] demonstrate much better performance, achieving an average error of less than 1%. In particular, FLUTE (A = 18) and REST (T = 8) perform strongly in all these instances. Building on this strong foundation, OAREST surpasses other baselines on R5–R40 instances and achieves competitive performance on R45 and R50. A visualized example of a 50-pin instance is shown in Fig. 4(a).

The advantages of OAREST are even more pronounced in terms of runtime. In line with the setup in [5], we adopt a batch size of $100\,\mathrm{k}/\textit{degree}$ for inference. As illustrated in Fig. 3, while GeoSteiner produces optimal results, its runtime grows exponentially with the number of pins. FLUTE (A = 18) offers significantly better efficiency than GeoSteiner, but its runtime still increases considerably as the number of pins grows. In contrast, the inference time of OAREST scales almost linearly with the number of pins, slightly exceeding that of REST. The additional time mainly stems from the inspection of obstacles. Note that while REST performs pretty well in both wirelength and runtime, it struggles with the multi-degree inference problem. This limitation results in a sharp increase in runtime when dealing with variable pin counts in real-world circuits. We will further investigate this issue in Sec. 4.4.

4.3 Main Results of OARSMT

We evaluate the wirelength, overlap, and runtime of GeoSteiner, OARST, ObSteiner, and OAREST in Fig. 5, where GeoSteiner [16] and ObSteiner [21] are used as the exact solvers for the RSMT and OARSMT problems, respectively. OARST implemented by [20] serves as an approximation solution for OARSMT. In this setting, we randomly add 5 and 10 obstacles to R5-R50 test cases proposed by [5], using a full batch size of $10\,\mathrm{k}$. Fig. 4(b) visualizes an instance with 20 pins and 10 obstacles.

In Fig. 5(a), all algorithms, including the exact OARSMT solver, have a gap compared to GeoSteiner due to the additional complexity of accounting for overlaps. While the wirelength achieved by OAREST is slightly longer than that of the exact OARSMT solution, it demonstrates a clear advantage over the approximation-based OARST.

Table 4: Average percentage error (%) of RSMTs compared to the exact algorithm GeoSteiner [16]. Best results except GeoSteiner are in **bold**.

Instances	GeoSteiner [16]	R-MST [17]	BGA [18]	FLUTE [19]		REST [5]		OAREST (ours)
				A = 3*	A = 18*	T = 1*	T = 8*	
R5	0.00	10.91	0.23	**0.00**	**0.00**	0.02	**0.00**	**0.00** ± **0.000**
R10	0.00	11.96	0.48	0.12	0.04	0.23	**0.01**	**0.01** ± **0.000**
R15	0.00	12.19	0.53	0.55	0.06	0.45	**0.03**	**0.03** ± **0.001**
R20	0.00	12.41	0.57	1.03	0.11	0.56	0.07	**0.06** ± **0.001**
R25	0.00	12.47	0.58	1.44	0.18	0.69	0.12	**0.10** ± **0.001**
R30	0.00	12.56	0.60	1.83	0.23	0.77	0.16	**0.15** ± **0.004**
R35	0.00	12.63	0.62	2.13	0.26	0.84	0.21	**0.19** ± **0.002**
R40	0.00	12.65	0.63	1.05	0.29	0.86	0.25	**0.24** ± **0.001**
R45	0.00	12.67	0.63	1.07	**0.30**	0.98	0.32	0.31 ± 0.002
R50	0.00	12.72	0.64	1.12	**0.29**	1.01	0.36	0.36 ± 0.001

* A=3/18 and T=1/8 are different versions of FLUTE and REST, which we illustrate in Appendix B.2.

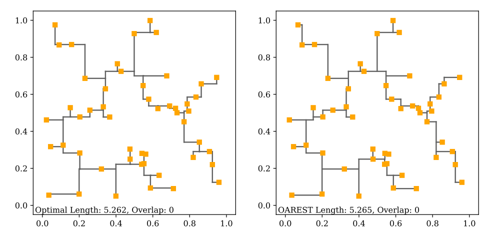
Optimal Length: 5.262, Overlap: 0
OAREST Length: 5.265, Overlap: 0

(a) RSMT with 50 pins.

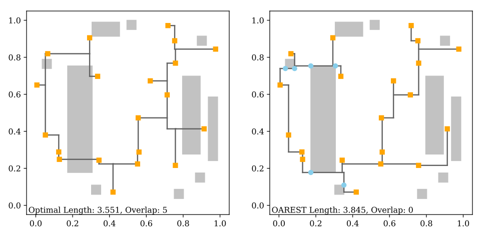
Optimal Length: 3.551, Overlap: 5
OAREST Length: 3.845, Overlap: 0

(b) OARSMT with 20 pins and 10 obstacles.

Figure 4: a) A pair of RSMTs with 50 pins, and b) a pair of OARSMTs with 20 pins and 10 obstacles, respectively run by the optimal GeoSteiner (left of each pair) and OAREST (right of each pair).

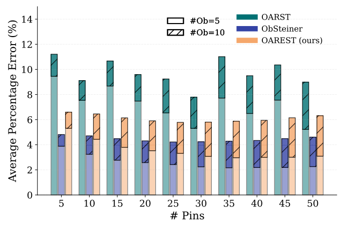

(a) Wirelength.

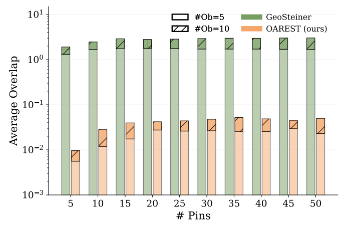

(b) Overlap (log-axis).

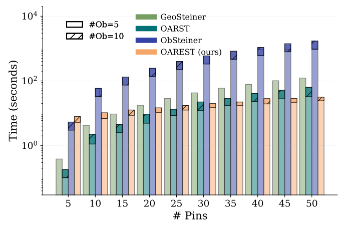

(c) Time (log-axis).

Figure 5: a) Average percentage error on task OARSMT compared to GeoSteiner; b) Average overlap on task OARSMT of GeoSteiner and OAREST; c) Time overhead on task OARSMT of GeoSteiner, OARST, ObSteiner, and OAREST.

Fig. 5(b) shows the average overlaps produced by GeoSteiner and OAREST. As GeoSteiner does not consider obstacles, it inherently suffers from significant overlaps. OAREST, on the contrary, reduces the overlap to a negligible level. Specifically, OAREST achieves >98%/96% success rates (zero-overlap solutions) for instances with 5/10 obstacles, respectively. Detailed statistics can be achieved in Appendix B.1. Such success rates are significant, as no obstacle is visible during the training stage. The small proportion of failed cases (1-4%) typically have minor overlaps in few rectilinear edges after performing OAREST. These can be resolved using maze routing postprocessing [22, 23] with <1% additional runtime compared to OAREST's inference time, maintaining practical feasibility while preserving computational advantages. We leave further reduction of overlaps as future work.

In Fig. 5(c), we compare the time overhead of the four algorithms. Unsurprisingly, the exact OARSMT solver (ObSteiner) has the highest computational cost, reflecting the inherent complexity of solving OARSMT problems exactly. The approximation solution, OARST, achieves a faster runtime than GeoSteiner. Importantly, we are delighted to see that OAREST outperforms all baselines in most instances, with its runtime being minimally affected by the presence of obstacles. This efficiency is attributed to the GPU parallelization capabilities and the linear scalability of OAREST with respect to obstacle handling.

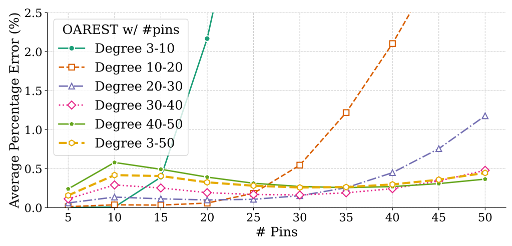

(a) Performance trained on varied degrees.

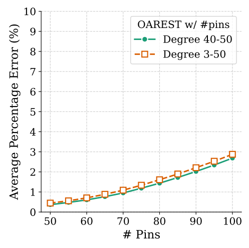

(b) Generality.

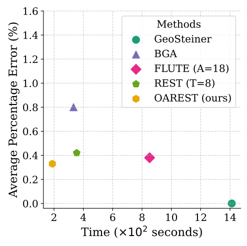

(c) Error/Time.

Figure 6: a) Average percentage error of OAREST trained on a varied range of degrees. b) Average percentage error of OAREST $(40-50)$ and OAREST $(3-50)$ on random instances with degrees $50-100$. c) Experiments on ICCAD19 global routing benchmark.

4.4 Other Experiments

Ablation Studies. Equipped with the dynamic masking strategies, OAREST is capable of training or inferring across a varied range of degrees. Our training strategy first follows REST [5] that trains on a single degree one by one, and is then followed by a quick finetuning process jointly across a range of degrees, including $(3, 10)$, $(10, 20)$, $(20, 30)$, $(30, 40)$, $(40, 50)$, and the full range of $(3, 50)$. As shown in Fig. 6(a), OAREST (3 - 50) has a robust performance on all degrees; however, the highest accuracy is consistently achieved by models trained specifically on smaller, targeted ranges of degrees. For instance, though OAREST (3 - 10) performs poorly on large degrees (15 - 50), it ranks first for degrees 5 and 10. This empirical observation could offer users the flexibility to balance parallel inference and accuracy.

Generality on Untrained Degrees. OAREST has a strong capability to extend to untrained degrees. To evaluate this, we tested OAREST (40–50) and OAREST (3–50) on RSMT instances with degrees between 50 and 100. As shown in Fig. 6(b), the average percentage error for both models increases as the number of pins grows. However, even for degrees $51-100$, which were not included in the training process, the error remains below 3%, highlighting the robustness of OAREST in handling unseen degrees.

Evaluation on Real-world Circuits. We evaluated OAREST on the ICCAD19 global routing [15] benchmark. In line with REST [5], we focused on instances with degrees between 3 and 100, as instances with degrees > 100 constitute only 0.002% of the dataset (see Table 3). In Fig. 6(c), OAREST outperforms baselines in efficiency with the second-best wirelength (inferior to the exact algorithm GeoSteiner). The time of OAREST is nearly half that of REST (T=8) and 1/7 of GeoSteiner, showing the scalability on real-world benchmarks.

5 Related Work

5.1 Rectilinear Steiner Minimum Tree (RSMT)

Rectilinear Steiner Minimum Tree (RSMT) algorithms can be mainly divided into approximation, heuristics, and machine learning (ML). Early approximation approaches target near-optimal solutions with efficiency, including R-MST [17] providing 1.5-approximation, [24] approaching 1.25-approximation, and Arora [25] providing $(1+\varepsilon)$-approximation. Apart from these methods, heuristic-based approaches achieve greater efficiency and accuracy, where BGA [18] utilizes heuristics to optimize edges based on the pre-computed R-MSTs. FLUTE [26, 19], a widely used industrial tool, leverages a lookup table for small instances with ≤ 9 pins and partitions larger instances into smaller sets for processing. GeoSteiner [16] is also heuristic-based but achieves exact solutions by generating all candidate Steiner Trees.

ML-based methods, especially reinforcement learning (RL), are used for constructing Steiner trees in RSMT. REST [5] proposes the rectilinear edge sequence (RES) and an RL framework based on actor-critic networks to generate the edge sequence, and EPST [6] extends the problem to Octilinear Steiner Minimum Tree (OSMT). Moreover, HubRouter [2] applies the RL-based RSMT to global routing problems. NN-Steiner [27] utilizes four neural network components to replace the consuming dynamic programming in [25].

Apart from the ability to handle obstacles, our OAREST addresses the multi-degree GPU parallelization in current RL-based methods, which is crucial in VLSI designs.

5.2 Obstacle-Avoiding Rectilinear Steiner Minimum Tree (OARSMT)

Based on the vanilla RSMT problems, various works study the strategies to avoid obstacles. Traditional solutions [22, 23] propose heuristic approaches based on maze routing, while EBOARST [28] utilizes a four-step algorithm to efficiently handle obstacles. FOARS [29] addresses obstacles based on FLUTE [26]. [20] proposes an OARSMT algorithm by sequentially using OASG, and OARST, achieving improved wirelength. Moreover, GSLS [30] proposes a guiding solution-based local search method to solve the OARSMT problem, while [31] focuses on selecting Steiner points to handle obstacles. Apart from the approximation and heuristic algorithms, exact algorithms of OARSMT include [32, 33, 34, 21], which study edge-disjoint full Steiner trees (FSTs) building upon the GeoSteiner [16] in vanilla RSMT.

Similar to RSMT problems, RL is also widely used in OARSMT. For instance, [9] utilizes an RL agent to select Steiner points and follows a Maze-router-based Prim's algorithm to form an OARSMT. [7] trains an RL agent based on the small grids of layouts and predicts the Steiner points. It also depends on a Maze routing as postprocessing. [8] performs a fast RL agent to connect pins, but it requires the pre-construction of Obstacle-Avoiding Spanning Graph (OASG) and separates it into shortest path forest (SPF), and finally, a local optimization strategy is employed for postprocessing.

Though these RL-based OARSMT algorithms can effectively handle obstacles, they either suffer from a large action space [7] or combine with heuristics [8, 9], lacking the efficiency of GPU parallelization.

5.3 Beyond RSMT in VLSI design

Beyond RSMT, various works in VLSI design employ reinforcement learning (RL) to address specific problems. For example, MaskPlace [35] uses RL to place macros sequentially during placement. Beyond macro placement, MaskRegulate [36] uses an RL policy to adjust existing layouts with dense rewards. Additionally, HAVE [37] introduces hierarchical adaptive multi-task RL and achieves higher hypervolume. In floorplanning, CBL [38] designs a floorplanner using the Corner Block List representation under an RL framework. Also within an RL framework, FlexPlanner [39] extends the problem to 3D floorplanning. For routing, Liao et al. [40] employ a deep Q-network (DQN) for global routing. Note that RSMT is an essential subproblem in routing, where we envision that OAREST makes a promising contribution.

Beyond VLSI design, combinatorial optimization problems form the fundamental basis of various applications, such as molecule generation [41, 42] and protein-protein docking [43]. Within the domain of EDA, our work provides a train-and-test perspective on generalization, specifically regarding varying degrees and obstacle constraints.

6 Conclusion and Outlook

We have introduced an RL-based OARSMT solver that supports multi-degree parallel inference and dynamic obstacle avoidance. The main contributions of this work include the theoretical demonstration of the optimality of the rectilinear edge sequence (RES) in OARSMT problems, as well as empirical validation on both synthetic and real-world benchmarks.

Despite its strengths, OAREST has some limitations that present potential areas for future research: 1) In instances with a large number of pins, the error in OAREST increases due to its training being limited to degrees between 3 and 50. 2) In some extreme scenarios, overlaps may still occur with OAREST. To address these issues, we propose the following directions for future work: 1) Training OAREST on instances with obstacles to further improve its ability to avoid obstacles while maintaining minimal wirelength; 2) Testing OAREST on more complex real-world global routing datasets and incorporating additional constraints, such as overflow; 3) Developing methods to completely eliminate overlaps in OARSMT problems.

References

[1] Sheng-En David Lin and Dae Hyun Kim. Construction of all rectilinear steiner minimum trees on the hanan grid and its applications to vlsi design. *IEEE Transactions on Computer-Aided Design of Integrated Circuits and Systems*, 39(6):1165–1176, 2019.

[2] Xingbo Du, Chonghua Wang, Ruizhe Zhong, and Junchi Yan. Hubrouter: Learning global routing via hub generation and pin-hub connection. *Advances in Neural Information Processing Systems*, 36:1–10, 2023.

[3] Ruizhi Liu, ZhishengZeng, Shizhe Ding, Jingyan Sui, Xingquan Li, and Dongbo Bu. Neuralsteiner: Learning steiner tree for overflow-avoiding global routing in chip design. In *The Thirty-eighth Annual Conference on Neural Information Processing Systems*, 2024.

[4] Michael R Garey and David S. Johnson. The rectilinear steiner tree problem is np-complete. *SIAM Journal on Applied Mathematics*, 32(4):826–834, 1977.

[5] Jinwei Liu, Gengjie Chen, and Evangeline FY Young. Rest: Constructing rectilinear steiner minimum tree via reinforcement learning. In *2021 58th ACM/IEEE Design Automation Conference (DAC)*, pages 1135–1140. IEEE, 2021.

[6] Zhenkun Lin, Genggeng Liu, Xing Huang, Yibo Lin, Jixin Zhang, Wen-Hao Liu, and Ting-Chi Wang. A unified deep reinforcement learning approach for constructing rectilinear and octilinear steiner minimum tree. *IEEE Transactions on Computer-Aided Design of Integrated Circuits and Systems*, 2024.

[7] Po-Yan Chen, Bing-Ting Ke, Tai-Cheng Lee, I-Ching Tsai, Tai-Wei Kung, Li-Yi Lin, En-Cheng Liu, Yun-Chih Chang, Yih-Lang Li, and Mango C-T Chao. A reinforcement learning agent for obstacle-avoiding rectilinear steiner tree construction. In *Proceedings of the 2022 international symposium on physical design*, pages 107–115, 2022.

[8] Zhenkun Lin, Yuhan Zhu, Xing Huang, Liliang Yang, and Genggeng Liu. Obstacle-avoiding rectilinear steiner minimal tree algorithm based on deep reinforcement learning. In *2023 International Conference on Artificial Intelligence of Things and Systems (AIoTSys)*, pages 149–156. IEEE, 2023.

[9] Liang-Ting Chen, Hung-Ru Kuo, Yih-Lang Li, and Mango C-T Chao. Arbitrary-size multi-layer oarsmt rl router trained with combinatorial monte-carlo tree search. In *Proceedings of the 61st ACM/IEEE Design Automation Conference*, pages 1–6, 2024.

[10] Zijie Geng, Jie Wang, Ziyan Liu, Siyuan Xu, Zhentao Tang, Shixiong Kai, Mingxuan Yuan, Jianye HAO, and Feng Wu. LaMPlace: Learning to optimize cross-stage metrics in macro placement. In *The Thirteenth International Conference on Learning Representations*, 2025.

[11] Pengyi Li, YAN ZHENG, Hongyao Tang, Xian Fu, and Jianye HAO. Evorainbow: Combining improvements in evolutionary reinforcement learning for policy search. In *Forty-first International Conference on Machine Learning*, 2024.

[12] Zijie Geng, Jie Wang, Ziyan Liu, Siyuan Xu, Zhentao Tang, Mingxuan Yuan, Jianye HAO, Yongdong Zhang, and Feng Wu. Reinforcement learning within tree search for fast macro placement. In *Forty-first International Conference on Machine Learning*, 2024.

[13] Yao Lai, Jinxin Liu, Zhentao Tang, Bin Wang, Jianye Hao, and Ping Luo. ChiPFormer: Transferable chip placement via offline decision transformer. In Andreas Krause, Emma Brunskill, Kyunghyun Cho, Barbara Engelhardt, Sivan Sabato, and Jonathan Scarlett, editors, *Proceedings of the 40th International Conference on Machine Learning*, volume 202 of *Proceedings of Machine Learning Research*, pages 18346–18364. PMLR, 23–29 Jul 2023.

[14] Ronald J Williams. Simple statistical gradient-following algorithms for connectionist reinforcement learning. *Machine learning*, 1992.

[15] Sergei Dolgov, Alexander Volkov, Lutong Wang, and Bangqi Xu. 2019 cad contest: Lef/def based global routing. In *2019 IEEE/ACM International Conference on Computer-Aided Design (ICCAD)*, pages 1–4. IEEE, 2019.

[16] David Michael Warme. *Spanning trees in hypergraphs with applications to Steiner trees*. University of Virginia, 1998.

[17] Frank K Hwang. An o (n log n) algorithm for rectilinear minimal spanning trees. *Journal of the ACM (JACM)*, 26(2):177–182, 1979.

[18] Andrew B Kahng, Ion I Măndoiu, and Alexander Z Zelikovsky. Highly scalable algorithms for rectilinear and octilinear steiner trees. In *Proceedings of the 2003 Asia and South Pacific Design Automation Conference*, pages 827–833, 2003.

[19] Yiu-Chung Wong and Chris Chu. A scalable and accurate rectilinear steiner minimal tree algorithm. In *2008 IEEE International Symposium on VLSI Design, Automation and Test (VLSI-DAT)*, pages 29–34. IEEE, 2008.

[20] Chung-Wei Lin, Szu-Yu Chen, Chi-Feng Li, Yao-Wen Chang, and Chia-Lin Yang. Efficient obstacle-avoiding rectilinear steiner tree construction. In *Proceedings of the 2007 international symposium on Physical design*, pages 127–134, 2007.

[21] Tao Huang and Evangeline FY Young. Obsteiner: An exact algorithm for the construction of rectilinear steiner minimum trees in the presence of complex rectilinear obstacles. *IEEE Transactions on Computer-Aided Design of Integrated Circuits and Systems*, 32(6):882–893, 2013.

[22] Liang Li and Evangeline FY Young. Obstacle-avoiding rectilinear steiner tree construction. In *2008 IEEE/ACM International Conference on Computer-Aided Design*, pages 523–528. IEEE, 2008.

[23] Kuen-Wey Lin, Yeh-Sheng Lin, Yih-Lang Li, and Rung-Bin Lin. A maze routing-based methodology with bounded exploration and path-assessed retracing for constrained multilayer obstacle-avoiding rectilinear steiner tree construction. *ACM Transactions on Design Automation of Electronic Systems (TODAES)*, 23(4):1–26, 2018.

[24] Piotr Berman, Ulrich Fößmeier, Marek Karpinski, Michael Kaufmann, and Alexander Zelikovsky. Approaching the 5/4—approximation for rectilinear steiner trees. In *Algorithms—ESA'94: Second Annual European Symposium Utrecht, The Netherlands, September 26–28, 1994 Proceedings 2*, pages 60–71. Springer, 1994.

[25] Sanjeev Arora. Polynomial time approximation schemes for euclidean traveling salesman and other geometric problems. *Journal of the ACM (JACM)*, 45(5):753–782, 1998.

[26] Chris Chu. Flute: Fast lookup table based wirelength estimation technique. In *IEEE/ACM International Conference on Computer Aided Design, 2004. ICCAD-2004.*, pages 696–701. IEEE, 2004.

[27] Andrew B Kahng, Robert R Nerem, Yusu Wang, and Chien-Yi Yang. Nn-steiner: A mixed neural-algorithmic approach for the rectilinear steiner minimum tree problem. In *Proceedings of the AAAI Conference on Artificial Intelligence*, volume 38, pages 13022–13030, 2024.

[28] Jieyi Long, Hai Zhou, and Seda Ogrenci Memik. Eboarst: An efficient edge-based obstacle-avoiding rectilinear steiner tree construction algorithm. *IEEE Transactions on Computer-Aided Design of Integrated Circuits and Systems*, 27(12):2169–2182, 2008.

[29] Gaurav Ajwani, Chris Chu, and Wai-Kei Mak. Foars: Flute based obstacle-avoiding rectilinear steiner tree construction. In *Proceedings of the 19th international symposium on Physical design*, pages 27–34, 2010.

[30] Tiancheng Zhang, Zhipeng Lü, and Junwen Ding. Guiding solution based local search for obstacle-avoiding rectilinear steiner minimal tree problem. *IEEE Transactions on Emerging Topics in Computational Intelligence*, 2023.

[31] Chih-Hung Liu, Sy-Yen Kuo, DT Lee, Chun-Syun Lin, Jung-Hung Weng, and Shih-Yi Yuan. Obstacle-avoiding rectilinear steiner tree construction: A steiner-point-based algorithm. *IEEE Transactions on Computer-Aided Design of Integrated Circuits and Systems*, 31(7):1050–1060, 2012.

[32] Liang Li, Zaichen Qian, and Evangeline FY Young. Generation of optimal obstacle-avoiding rectilinear steiner minimum tree. In *Proceedings of the 2009 International Conference on Computer-Aided Design*, pages 21–25, 2009.

[33] Tao Huang and Evangeline FY Young. Obstacle-avoiding rectilinear steiner minimum tree construction: An optimal approach. In *2010 IEEE/ACM International Conference on Computer-Aided Design (ICCAD)*, pages 610–613. IEEE, 2010.

[34] Tao Huang, Liang Li, and Evangeline FY Young. On the construction of optimal obstacle-avoiding rectilinear steiner minimum trees. *IEEE transactions on computer-aided design of integrated circuits and systems*, 30(5):718–731, 2011.

[35] Yao Lai, Yao Mu, and Ping Luo. Maskplace: Fast chip placement via reinforced visual representation learning. *Advances in Neural Information Processing Systems*, 35:24019–24030, 2022.

[36] Ke Xue, Ruo-Tong Chen, Xi Lin, Yunqi Shi, Shixiong Kai, Siyuan Xu, and Chao Qian. Reinforcement learning policy as macro regulator rather than macro placer. *Advances in Neural Information Processing Systems*, 37:140565–140588, 2024.

[37] Zhihai Wang, Jie Wang, Dongsheng Zuo, Ji Yunjie, Xilin Xia, Yuzhe Ma, Jianye Hao, Mingxuan Yuan, Yongdong Zhang, and Feng Wu. A hierarchical adaptive multi-task reinforcement learning framework for multiplier circuit design. In *Forty-first International Conference on Machine Learning*, 2024.

[38] Mohammad Amini, Zhanguang Zhang, Surya Penmetsa, Yingxue Zhang, Jianye Hao, and Wulong Liu. Generalizable floorplanner through corner block list representation and hypergraph embedding. In *Proceedings of the 28th ACM SIGKDD conference on knowledge discovery and data mining*, pages 2692–2702, 2022.

[39] Ruizhe Zhong, Xingbo Du, Shixiong Kai, Zhentao Tang, Siyuan Xu, Jianye Hao, Mingxuan Yuan, and Junchi Yan. Flexplanner: Flexible 3d floorplanning via deep reinforcement learning in hybrid action space with multi-modality representation. *Advances in Neural Information Processing Systems*, 37:49252–49278, 2024.

[40] Haiguang Liao, Wentai Zhang, Xuliang Dong, Barnabas Poczos, Kenji Shimada, and Levent Burak Kara. A deep reinforcement learning approach for global routing. *Journal of Mechanical Design*, 142(6):061701, 2020.

[41] Huanjin Wu, Xinyu Ye, and Junchi Yan. Qvae-mole: The quantum vae with spherical latent variable learning for 3-d molecule generation. *Advances in Neural Information Processing Systems*, 37:22745–22771, 2024.

[42] Nianzu Yang, Huaijin Wu, Kaipeng Zeng, Yang Li, Siyuan Bao, and Junchi Yan. Molecule generation for drug design: a graph learning perspective. *Fundamental Research*, 2024.

[43] Huaijin Wu, Wei Liu, Yatao Bian, Jiaxiang Wu, Nianzu Yang, and Junchi Yan. Ebmdock: Neural probabilistic protein-protein docking via a differentiable energy model. In *The Twelfth International Conference on Learning Representations*, 2024.

[44] Maurice Hanan. On steiner's problem with rectilinear distance. *SIAM Journal on Applied mathematics*, 14(2):255–265, 1966.

[45] Frank K Hwang. On steiner minimal trees with rectilinear distance. *SIAM journal on Applied Mathematics*, 30(1):104–114, 1976.

[46] Sergey Ioffe. Batch normalization: Accelerating deep network training by reducing internal covariate shift. *arXiv preprint arXiv:1502.03167*, 2015.

[47] A Vaswani. Attention is all you need. *Advances in Neural Information Processing Systems*, 2017.

[48] Oriol Vinyals, Meire Fortunato, and Navdeep Jaitly. Pointer networks. *Advances in neural information processing systems*, 28, 2015.

[49] Diederik P Kingma. Adam: A method for stochastic optimization. *arXiv preprint arXiv:1412.6980*, 2014.

NeurIPS Paper Checklist

1. **Claims**

   Question: Do the main claims made in the abstract and introduction accurately reflect the paper's contributions and scope?

   Answer: [Yes]

   Justification: The main claims made in the abstract and introduction accurately reflect the paper's contributions and scope.

   Guidelines:

   - The answer NA means that the abstract and introduction do not include the claims made in the paper.
   - The abstract and/or introduction should clearly state the claims made, including the contributions made in the paper and important assumptions and limitations. A No or NA answer to this question will not be perceived well by the reviewers.
   - The claims made should match theoretical and experimental results, and reflect how much the results can be expected to generalize to other settings.
   - It is fine to include aspirational goals as motivation as long as it is clear that these goals are not attained by the paper.

2. **Limitations**

   Question: Does the paper discuss the limitations of the work performed by the authors?

   Answer: [Yes]

   Justification: This paper discusses the limitations in the conclusion section.

   Guidelines:

   - The answer NA means that the paper has no limitation while the answer No means that the paper has limitations, but those are not discussed in the paper.
   - The authors are encouraged to create a separate "Limitations" section in their paper.
   - The paper should point out any strong assumptions and how robust the results are to violations of these assumptions (e.g., independence assumptions, noiseless settings, model well-specification, asymptotic approximations only holding locally). The authors should reflect on how these assumptions might be violated in practice and what the implications would be.
   - The authors should reflect on the scope of the claims made, e.g., if the approach was only tested on a few datasets or with a few runs. In general, empirical results often depend on implicit assumptions, which should be articulated.
   - The authors should reflect on the factors that influence the performance of the approach. For example, a facial recognition algorithm may perform poorly when image resolution is low or images are taken in low lighting. Or a speech-to-text system might not be used reliably to provide closed captions for online lectures because it fails to handle technical jargon.
   - The authors should discuss the computational efficiency of the proposed algorithms and how they scale with dataset size.
   - If applicable, the authors should discuss possible limitations of their approach to address problems of privacy and fairness.
   - While the authors might fear that complete honesty about limitations might be used by reviewers as grounds for rejection, a worse outcome might be that reviewers discover limitations that aren't acknowledged in the paper. The authors should use their best judgment and recognize that individual actions in favor of transparency play an important role in developing norms that preserve the integrity of the community. Reviewers will be specifically instructed to not penalize honesty concerning limitations.

3. **Theory assumptions and proofs**

   Question: For each theoretical result, does the paper provide the full set of assumptions and a complete (and correct) proof?

   Answer: [Yes]

Justification: This paper provides complete assumptions and proofs.

Guidelines:

- The answer NA means that the paper does not include theoretical results.
- All the theorems, formulas, and proofs in the paper should be numbered and cross-referenced.
- All assumptions should be clearly stated or referenced in the statement of any theorems.
- The proofs can either appear in the main paper or the supplemental material, but if they appear in the supplemental material, the authors are encouraged to provide a short proof sketch to provide intuition.
- Inversely, any informal proof provided in the core of the paper should be complemented by formal proofs provided in appendix or supplemental material.
- Theorems and Lemmas that the proof relies upon should be properly referenced.

4. **Experimental result reproducibility**

   Question: Does the paper fully disclose all the information needed to reproduce the main experimental results of the paper to the extent that it affects the main claims and/or conclusions of the paper (regardless of whether the code and data are provided or not)?

   Answer: [Yes]

   Justification: This paper provides experimental details, and particularly, the code is provided.

   Guidelines:

   - The answer NA means that the paper does not include experiments.
   - If the paper includes experiments, a No answer to this question will not be perceived well by the reviewers: Making the paper reproducible is important, regardless of whether the code and data are provided or not.
   - If the contribution is a dataset and/or model, the authors should describe the steps taken to make their results reproducible or verifiable.
   - Depending on the contribution, reproducibility can be accomplished in various ways. For example, if the contribution is a novel architecture, describing the architecture fully might suffice, or if the contribution is a specific model and empirical evaluation, it may be necessary to either make it possible for others to replicate the model with the same dataset, or provide access to the model. In general. releasing code and data is often one good way to accomplish this, but reproducibility can also be provided via detailed instructions for how to replicate the results, access to a hosted model (e.g., in the case of a large language model), releasing of a model checkpoint, or other means that are appropriate to the research performed.
   - While NeurIPS does not require releasing code, the conference does require all submissions to provide some reasonable avenue for reproducibility, which may depend on the nature of the contribution. For example
     (a) If the contribution is primarily a new algorithm, the paper should make it clear how to reproduce that algorithm.
     (b) If the contribution is primarily a new model architecture, the paper should describe the architecture clearly and fully.
     (c) If the contribution is a new model (e.g., a large language model), then there should either be a way to access this model for reproducing the results or a way to reproduce the model (e.g., with an open-source dataset or instructions for how to construct the dataset).
     (d) We recognize that reproducibility may be tricky in some cases, in which case authors are welcome to describe the particular way they provide for reproducibility. In the case of closed-source models, it may be that access to the model is limited in some way (e.g., to registered users), but it should be possible for other researchers to have some path to reproducing or verifying the results.

5. **Open access to data and code**

   Question: Does the paper provide open access to the data and code, with sufficient instructions to faithfully reproduce the main experimental results, as described in supplemental material?

Answer: [Yes]

Justification: All the data used in this paper are open-sourced, and the code is provided in the GitHub link.

Guidelines:

- The answer NA means that paper does not include experiments requiring code.
- Please see the NeurIPS code and data submission guidelines (https://nips.cc/public/guides/CodeSubmissionPolicy) for more details.
- While we encourage the release of code and data, we understand that this might not be possible, so "No" is an acceptable answer. Papers cannot be rejected simply for not including code, unless this is central to the contribution (e.g., for a new open-source benchmark).
- The instructions should contain the exact command and environment needed to run to reproduce the results. See the NeurIPS code and data submission guidelines (https://nips.cc/public/guides/CodeSubmissionPolicy) for more details.
- The authors should provide instructions on data access and preparation, including how to access the raw data, preprocessed data, intermediate data, and generated data, etc.
- The authors should provide scripts to reproduce all experimental results for the new proposed method and baselines. If only a subset of experiments are reproducible, they should state which ones are omitted from the script and why.
- At submission time, to preserve anonymity, the authors should release anonymized versions (if applicable).
- Providing as much information as possible in supplemental material (appended to the paper) is recommended, but including URLs to data and code is permitted.

6. **Experimental setting/details**

   Question: Does the paper specify all the training and test details (e.g., data splits, hyper-parameters, how they were chosen, type of optimizer, etc.) necessary to understand the results?

   Answer: [Yes]

   Justification: This paper provides details of the experimental protocols and ablation studies.

   Guidelines:

   - The answer NA means that the paper does not include experiments.
   - The experimental setting should be presented in the core of the paper to a level of detail that is necessary to appreciate the results and make sense of them.
   - The full details can be provided either with the code, in appendix, or as supplemental material.

7. **Experiment statistical significance**

   Question: Does the paper report error bars suitably and correctly defined or other appropriate information about the statistical significance of the experiments?

   Answer: [Yes]

   Justification: This paper reports the standard deviation of the average percentage error.

   Guidelines:

   - The answer NA means that the paper does not include experiments.
   - The authors should answer "Yes" if the results are accompanied by error bars, confidence intervals, or statistical significance tests, at least for the experiments that support the main claims of the paper.
   - The factors of variability that the error bars are capturing should be clearly stated (for example, train/test split, initialization, random drawing of some parameter, or overall run with given experimental conditions).
   - The method for calculating the error bars should be explained (closed form formula, call to a library function, bootstrap, etc.)
   - The assumptions made should be given (e.g., Normally distributed errors).

- It should be clear whether the error bar is the standard deviation or the standard error of the mean.
- It is OK to report 1-sigma error bars, but one should state it. The authors should preferably report a 2-sigma error bar than state that they have a 96% CI, if the hypothesis of Normality of errors is not verified.
- For asymmetric distributions, the authors should be careful not to show in tables or figures symmetric error bars that would yield results that are out of range (e.g. negative error rates).
- If error bars are reported in tables or plots, The authors should explain in the text how they were calculated and reference the corresponding figures or tables in the text.

8. **Experiments compute resources**

   Question: For each experiment, does the paper provide sufficient information on the computer resources (type of compute workers, memory, time of execution) needed to reproduce the experiments?

   Answer: [Yes]

   Justification: This paper provides a detailed introduction to computing resources.

   Guidelines:

   - The answer NA means that the paper does not include experiments.
   - The paper should indicate the type of compute workers CPU or GPU, internal cluster, or cloud provider, including relevant memory and storage.
   - The paper should provide the amount of compute required for each of the individual experimental runs as well as estimate the total compute.
   - The paper should disclose whether the full research project required more compute than the experiments reported in the paper (e.g., preliminary or failed experiments that didn't make it into the paper).

9. **Code of ethics**

   Question: Does the research conducted in the paper conform, in every respect, with the NeurIPS Code of Ethics `https://neurips.cc/public/EthicsGuidelines`?

   Answer: [Yes]

   Justification: This research conforms with the NeurIPS Code of Ethics.

   Guidelines:

   - The answer NA means that the authors have not reviewed the NeurIPS Code of Ethics.
   - If the authors answer No, they should explain the special circumstances that require a deviation from the Code of Ethics.
   - The authors should make sure to preserve anonymity (e.g., if there is a special consideration due to laws or regulations in their jurisdiction).

10. **Broader impacts**

    Question: Does the paper discuss both potential positive societal impacts and negative societal impacts of the work performed?

    Answer: [Yes]

    Justification: As shown in the introduction, this paper presents work whose goal is to advance the field of Machine Learning and the field of Artificial Intelligence for Electronic Design Automation (AI4EDA). Its negative impact is shown in the conclusion.

    Guidelines:

    - The answer NA means that there is no societal impact of the work performed.
    - If the authors answer NA or No, they should explain why their work has no societal impact or why the paper does not address societal impact.
    - Examples of negative societal impacts include potential malicious or unintended uses (e.g., disinformation, generating fake profiles, surveillance), fairness considerations (e.g., deployment of technologies that could make decisions that unfairly impact specific groups), privacy considerations, and security considerations.

- The conference expects that many papers will be foundational research and not tied to particular applications, let alone deployments. However, if there is a direct path to any negative applications, the authors should point it out. For example, it is legitimate to point out that an improvement in the quality of generative models could be used to generate deepfakes for disinformation. On the other hand, it is not needed to point out that a generic algorithm for optimizing neural networks could enable people to train models that generate Deepfakes faster.
- The authors should consider possible harms that could arise when the technology is being used as intended and functioning correctly, harms that could arise when the technology is being used as intended but gives incorrect results, and harms following from (intentional or unintentional) misuse of the technology.
- If there are negative societal impacts, the authors could also discuss possible mitigation strategies (e.g., gated release of models, providing defenses in addition to attacks, mechanisms for monitoring misuse, mechanisms to monitor how a system learns from feedback over time, improving the efficiency and accessibility of ML).

11. **Safeguards**

    Question: Does the paper describe safeguards that have been put in place for responsible release of data or models that have a high risk for misuse (e.g., pretrained language models, image generators, or scraped datasets)?

    Answer: [NA]

    Justification: This paper does not refer to data or models that have a high risk.

    Guidelines:

    - The answer NA means that the paper poses no such risks.
    - Released models that have a high risk for misuse or dual-use should be released with necessary safeguards to allow for controlled use of the model, for example by requiring that users adhere to usage guidelines or restrictions to access the model or implementing safety filters.
    - Datasets that have been scraped from the Internet could pose safety risks. The authors should describe how they avoided releasing unsafe images.
    - We recognize that providing effective safeguards is challenging, and many papers do not require this, but we encourage authors to take this into account and make a best faith effort.

12. **Licenses for existing assets**

    Question: Are the creators or original owners of assets (e.g., code, data, models), used in the paper, properly credited and are the license and terms of use explicitly mentioned and properly respected?

    Answer: [Yes]

    Justification: This paper follows the license when using existing assets.

    Guidelines:

    - The answer NA means that the paper does not use existing assets.
    - The authors should cite the original paper that produced the code package or dataset.
    - The authors should state which version of the asset is used and, if possible, include a URL.
    - The name of the license (e.g., CC-BY 4.0) should be included for each asset.
    - For scraped data from a particular source (e.g., website), the copyright and terms of service of that source should be provided.
    - If assets are released, the license, copyright information, and terms of use in the package should be provided. For popular datasets, `paperswithcode.com/datasets` has curated licenses for some datasets. Their licensing guide can help determine the license of a dataset.
    - For existing datasets that are re-packaged, both the original license and the license of the derived asset (if it has changed) should be provided.

- If this information is not available online, the authors are encouraged to reach out to the asset's creators.

13. **New assets**

    Question: Are new assets introduced in the paper well documented and is the documentation provided alongside the assets?

    Answer: [Yes]

    Justification: The new assets are well documented.

    Guidelines:

    - The answer NA means that the paper does not release new assets.
    - Researchers should communicate the details of the dataset/code/model as part of their submissions via structured templates. This includes details about training, license, limitations, etc.
    - The paper should discuss whether and how consent was obtained from people whose asset is used.
    - At submission time, remember to anonymize your assets (if applicable). You can either create an anonymized URL or include an anonymized zip file.

14. **Crowdsourcing and research with human subjects**

    Question: For crowdsourcing experiments and research with human subjects, does the paper include the full text of instructions given to participants and screenshots, if applicable, as well as details about compensation (if any)?

    Answer: [NA]

    Justification: This paper does not refer to research with human subjects.

    Guidelines:

    - The answer NA means that the paper does not involve crowdsourcing nor research with human subjects.
    - Including this information in the supplemental material is fine, but if the main contribution of the paper involves human subjects, then as much detail as possible should be included in the main paper.
    - According to the NeurIPS Code of Ethics, workers involved in data collection, curation, or other labor should be paid at least the minimum wage in the country of the data collector.

15. **Institutional review board (IRB) approvals or equivalent for research with human subjects**

    Question: Does the paper describe potential risks incurred by study participants, whether such risks were disclosed to the subjects, and whether Institutional Review Board (IRB) approvals (or an equivalent approval/review based on the requirements of your country or institution) were obtained?

    Answer: [NA]

    Justification: The paper does not involve crowdsourcing nor research with human subjects.

    Guidelines:

    - The answer NA means that the paper does not involve crowdsourcing nor research with human subjects.
    - Depending on the country in which research is conducted, IRB approval (or equivalent) may be required for any human subjects research. If you obtained IRB approval, you should clearly state this in the paper.
    - We recognize that the procedures for this may vary significantly between institutions and locations, and we expect authors to adhere to the NeurIPS Code of Ethics and the guidelines for their institution.
    - For initial submissions, do not include any information that would break anonymity (if applicable), such as the institution conducting the review.

16. **Declaration of LLM usage**

Question: Does the paper describe the usage of LLMs if it is an important, original, or non-standard component of the core methods in this research? Note that if the LLM is used only for writing, editing, or formatting purposes and does not impact the core methodology, scientific rigorousness, or originality of the research, declaration is not required.

Answer: [NA]

Justification: LLM is only used for editing in some parts.

Guidelines:

- The answer NA means that the core method development in this research does not involve LLMs as any important, original, or non-standard components.
- Please refer to our LLM policy (`https://neurips.cc/Conferences/2025/LLM`) for what should or should not be described.

A Theoretical Results

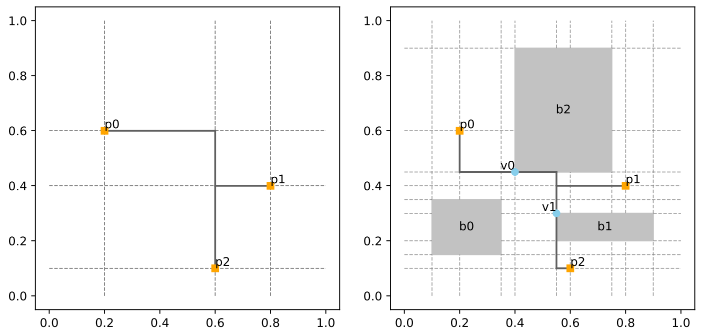

(a) Hanan Grid. (b) Extended Hanan Grid.

Figure 7: Visualization of a) Hanan Grid, and b) Extended Hanan Grid. The grids are shown as grey dashed lines.

A.1 Additional Definitions

In this section, we propose additional definitions apart from those in Sec. 2.1. The visualizations of Hanan Grid and Extended Hanan Grid are shown in Fig. 7(a) and Fig. 7(b).

Definition A.1. [Hanan Grid [44]]) For a given set of pins $\mathcal{P} = \{p_0, p_1, \cdots, p_{n-1}\}$, its Hanan grid $H(\mathcal{P})$ is defined as the grid composed of the intersection points of the horizontal and vertical lines of all pins. Formally,

$$H(\mathcal{P}) = \{(x, y) | x = x_i \text{ or } y = y_i, \forall p_i = (x_i, y_i)\} \tag{9}$$

Definition A.2. [Extended Hanan Grid] For a given set of pins $\mathcal{P} = \{p_0, p_1, \cdots, p_{n-1}\}$ and a set of rectangular obstacles $\mathcal{O} = \{o_0, o_1, \cdots, o_{m-1}\}$, its extended Hanan grid $H'(\mathcal{P}, \mathcal{O})$ is defined as the grid composed of the intersection points of the horizontal and vertical lines of all pins and the corners of all obstacles. Formally,

$$H'(\mathcal{P}, \mathcal{O}) = \{(x, y) | x = x_i \text{ or } y = y_i, \forall (x_i, y_i) \in \mathcal{P} \cup \mathcal{V}(\mathcal{O})\}, \tag{10}$$

where $\mathcal{V}(\mathcal{O})$ represents all corner vertices of obstacles $\mathcal{O}$.

A.2 Assumption and Lemma

In order to prove our main theorem in Sec. 2.3, we first put forward and prove some theoretical findings in this section. Though some theorems/lemmas originate from other works [44, 5], they lack corresponding proofs.

Assumption A.3. For a given set of pins $\mathcal{P} = \{p_0, p_1, \cdots, p_{n-1}\}$, its rectilinear edge sequence (RES) is valid iff. such RES connect all pins in $\mathcal{P}$.

Lemma A.4. *[Validity of RES] For a given set of pins $\mathcal{P} = \{p_0, p_1, \cdots, p_{n-1}\}$, its rectilinear edge sequence (RES) $res = ((v_0, h_0), (v_1, h_1), \cdots, (v_{n-2}, h_{n-2}))$ is guaranteed to be valid if*

1. *$v_0 \neq h_0$.*
2. *For each rectilinear edge pair (v_i, h_i) $(i \geq 1)$, exactly one of v_i, h_i is visited before by previous rectilinear edge pairs, and the other is not.*

Proof. The lemma obviously holds when $n = 3$. For $n > 3$, consider the construction process of RES. Since $v_0 \neq h_0$, the first pair contains two distinct points that are connected. For the i-th $(i \geq 1)$ pair, due to the second requirement, the newly-visited pin is connected to the previously-visited pins, and the number of connecting pins plus 1, and so forth, when $i = n - 2$, n pins are connected. □

Lemma A.5. *[Hanan's Theorem] For any set of pins $\mathcal{P} = \{p_0, p_1, \cdots, p_{n-1}\}$, there always exists an optimal Rectilinear Steiner Tree (RST), i.e., Rectilinear Steiner Minimum Tree (RSMT), that all Steiner points lie on the Hanan Grid.*

Proof. Suppose there exists an optimal RST that has a series of Steiner points $\mathcal{S} = \{s_0, s_1, \cdots, s_{j-1}\}$ not lying on the Hanan Grid. For each $s_i \in \mathcal{S}$, denote its coordinate as (x_i, y_i), then at least one of x_i, y_i is not equal to any of the pin coordinates.

Without loss of generality, we suppose x_i is not equal to any pin coordinates, then we move such Steiner point s_i to the nearest x-coordinate of pins. Due to the characteristic of Manhattan distance, after this movement, the length of the connection path referred to s_i is equal to the previous one.

Repeat the above process on all other Steiner points in $\mathcal{S}$, finally we obtain an optimal RST whose Steiner points are all on the Hanan Grid. □

Theorem A.6. ***[Optimality of RES]*** *For any set of pins $\mathcal{P} = \{p_0, p_1, \cdots, p_{n-1}\}$, an optimal RES of $\mathcal{P}$ can always be found such that its corresponding tree is an optimal RSMT for $\mathcal{P}$.*

Proof. Let T^* be an optimal RSMT for $\mathcal{P}$ with length L^*, and let $\mathcal{R}(\mathcal{P})$ be the set of all valid RES for $\mathcal{P}$. Denote by

$$r^* = \arg \min_{r \in \mathcal{R}(\mathcal{P})} \{\text{length}(T(r))\} \tag{11}$$

an optimal RES in $\mathcal{R}(\mathcal{P})$, where $T(r)$ is the corresponding tree of RES $r \in \mathcal{R}(\mathcal{P})$.

Suppose, for contradiction, that $\text{length}(T(r^*)) > L^*$.

By Lemma A.5, we may assume all Steiner points in T^* lie on the Hanan grid $H(\mathcal{P})$. Consider traversing T^* in a manner similar to a breadth-first search (BFS), starting from an arbitrary pin. Each time a new pin p_j is encountered, it is connected to an already visited pin p_i via a path that follows the Hanan grid and possibly passes through Steiner points.

Since all Steiner points are on the Hanan grid, the path from p_i to p_j consists of horizontal and vertical segments whose total length equals the Manhattan distance between p_i and p_j. Therefore, each such path can be represented as a direct sequence of horizontal and vertical edges between pins in the RES framework, implicitly accounting for any Steiner points.

Construct the RES r' by recording each connection (i, j) where p_j is connected to p_i. By construction:

1. Each edge (i, j) in r' corresponds to a rectilinear path in T^* with length equal to the Manhattan distance between p_i and p_j.
2. The sequence r' satisfies the conditions of Lemma A.4, ensuring that r' is a valid RES.
3. The total length of $T(r')$ equals L^* since each RES edge represents the minimal rectilinear distance required to connect p_j to the existing tree.

Thus, we have $r' \in \mathcal{R}(\mathcal{P})$ and $\text{length}(T(r')) = L^*$. This contradicts our assumption that $\text{length}(T(r^*)) > L^*$. Therefore, it must be that

$$\text{length}(T(r^*)) = L^*, \tag{12}$$

and r^* corresponds to an optimal RSMT. □

Lemma A.7. ***[Extended Hanan's Theorem]*** *For any set of pins $\mathcal{P} = \{p_0, p_1, \cdots, p_{n-1}\}$ and a set of rectangular obstacles $\mathcal{O} = \{o_0, o_1, \cdots, o_{m-1}\}$, there always exists an RSMT, that all Steiner points are lying on the extended Hanan Grid $H'(\mathcal{P}, \mathcal{O})$.*

Proof. The proof is similar to Lemma A.5. Suppose there exists an optimal RST that has a series of Steiner points $\mathcal{S} = \{s_0, s_1, \cdots, s_{j-1}\}$ not lying on Hanan Grid $H(\mathcal{P})$. For each $s_i \in \mathcal{S}$, denote its coordinate as (x_i, y_i), then at least one of x_i, y_i is not equal to any of the pin coordinates.

Without loss of generality, we suppose x_i is not equal to any of the coordinates of pins, then we try to move such Steiner point s_i to the nearest x-coordinate of pins. Consider two situations:

1. If the movement is successful, then the length of the connection path referred to s_i is equal to the previous one due to the characteristic of Manhattan distance.

2. If the movement fails (caused by obstacles), we can move s_i to the nearest x-coordinate of pins as far as possible until it is adjacent to an obstacle o_k. This operation will also not lead to longer length and the Steiner point s_i is moved to the extended Hanan Grid $H(\mathcal{P}, \mathcal{O})$.

Repeat the above process on all other Steiner points in $\mathcal{S}$, finally we obtain an optimal RST whose Steiner points are all on the extended Hanan Grid $H(\mathcal{P}, \mathcal{O})$.

Assumption A.8. For a given set of pins $\mathcal{P} = \{p_0, p_1, \cdots, p_{n-1}\}$ and a set of rectangular obstacles $\mathcal{O} = \{o_0, o_1, \cdots, o_{m-1}\}$, its rectilinear edge sequence (RES) r is valid iff.

1. Such RES connect all pins in $\mathcal{P}$.
2. $\forall edge \in r, \forall o_i \in \mathcal{O} : edge \cap \text{int}(o_i) = \emptyset$, where $\text{int}(o_i)$ denotes the interior region of obstacle o_i.

□

Lemma A.9. ***[Existence of valid RES in OARSMT]*** *For any set of pins $\mathcal{P} = \{p_0, p_1, \cdots, p_{n-1}\}$ and a set of rectangular obstacles $\mathcal{O} = \{o_0, o_1, \cdots, o_{m-1}\}$, suppose there exists a rectilinear Steiner tree (RST), then there always exists a subset of obstacles $\mathcal{V}'(\mathcal{O})$ and the corresponding valid rectilinear edge sequence (RES) of $\mathcal{P} \cup \mathcal{V}'(\mathcal{O})$.*

Proof. Clearly, it holds for the case without obstacles, so we only consider the case when RES overlaps with obstacles.

Define an empty set $\mathcal{U}$ and a RES r of $\mathcal{P}$. Suppose a rectilinear edge (v_i, h_i) in r overlaps with obstacle $o_j \in \mathcal{O}$, then we can choose an unvisited corner vertex u_j of obstacle o_j and divide (v_i, h_i) into $(v_i, u_j), (u_j, h_i)$.

Add u_j to $\mathcal{U}$ and replace (v_i, h_i) with two rectilinear edges $(v_i, u_j), (u_j, h_i)$ in r. Traverse all rectilinear edges until none of them overlap with any obstacle. Note that $\mathcal{U} \subset \mathcal{V}(\mathcal{O})$, so we denote $\mathcal{U} \triangleq \mathcal{V}'(\mathcal{O})$.

The split of (v_i, h_i) will simultaneously increase the number of rectilinear edges by 1 and the number of unvisited points by 1, so it satisfies the validity of RES stated in Lemma A.4.

□

A.3 Proof of the Main Theorem

Theorem A.10. ***[Optimality of RES in OARSMT]*** *For any set of pins $\mathcal{P} = \{p_0, p_1, \cdots, p_{n-1}\}$ and a set of rectangular obstacles $\mathcal{O} = \{o_0, o_1, \cdots, o_{m-1}\}$, an optimal RES of $\mathcal{P} \cup \mathcal{V}'(\mathcal{O})$ can always be found such that its corresponding tree is an optimal OARSMT for $\mathcal{P}$ under obstacles $\mathcal{O}$. Here, $\mathcal{V}'(\mathcal{O}) \subset \mathcal{V}(\mathcal{O})$ is a subset of the corner vertices of all obstacles.*

Proof. The proof is similar to that of Theorem A.6. Let T^* be an optimal OARSMT for $\mathcal{P}$ under obstacles $\mathcal{O}$ with length L^* and no overlaps, and let $\mathcal{R}(\mathcal{P}')$ be the set of all non-overlapping and valid RES for $\mathcal{P}' \triangleq \mathcal{P} \cup \mathcal{V}'(\mathcal{O})$. According to Lemma A.9, $\mathcal{R}(\mathcal{P}') \neq \emptyset$. Denote by

$$r^* = \arg\min_{r \in \mathcal{R}(\mathcal{P}')} \{\text{length}(T(r))\} \tag{13}$$

an optimal non-overlapping RES in $\mathcal{R}(\mathcal{P}')$, where $T(r)$ is the corresponding tree of RES $r \in \mathcal{R}(\mathcal{P}')$.

Suppose, for contradiction, that $\text{length}(T(r^*)) > L^*$.

By Lemma A.7, we may assume all Steiner points in T^* lie on the extended Hanan grid $H'(\mathcal{P}, \mathcal{O})$. Consider traversing T^* in a manner similar to a breadth-first search (BFS), starting from an arbitrary pin. Each time a new pin/vertex p_j is encountered, it is connected to an already visited pin/vertex p_i via a path that follows the extended Hanan grid and possibly passes through Steiner points.

Since all Steiner points are on the extended Hanan grid, the path from p_i to p_j consists of horizontal and vertical segments whose total length equals the Manhattan distance between p_i and p_j. Therefore, each such path can be represented as a direct sequence of horizontal and vertical edges between pins in the RES framework, implicitly accounting for any Steiner points.

Construct the RES r' by recording each connection (i, j) where p_j is connected to p_i. By construction:

1. Each edge (i, j) in r' corresponds to a rectilinear path in T^* with length equal to the Manhattan distance between p_i and p_j.
2. The sequence r' satisfies the conditions of Lemma A.4, ensuring that r' is a valid RES.
3. The total length of $T(r')$ equals L^* since each RES edge represents the minimal rectilinear distance required to connect p_j to the existing tree.

Thus, we have $r' \in \mathcal{R}(\mathcal{P}')$ and $\text{length}(T(r')) = L^*$. This contradicts our assumption that $\text{length}(T(r^*)) > L^*$. Therefore, it must be that

$$\text{length}(T(r^*)) = L^*, \tag{14}$$

and r^* corresponds to an optimal OARSMT. □

B Experiments

B.1 Success Rate

Table 5: Success rate (%) of GeoSteiner and OAREST on R5-R50 instances with 5/10 obstacles.

Instances	GeoSteiner		OAREST (ours)	
	5 Obstacles	10 Obstacles	5 Obstacles	10 Obstacles
R5	34.45	19.68	99.51	99.11
R10	27.65	13.60	98.55	97.64
R15	26.57	12.78	98.41	97.02
R20	28.03	12.03	98.06	96.38
R25	28.15	12.48	98.01	96.26
R30	29.75	11.37	98.14	96.44
R35	30.21	12.70	98.35	96.36
R40	30.37	12.10	98.35	96.52
R45	31.50	11.86	98.27	96.69
R50	32.29	11.98	98.57	96.71

We conduct success rates of GeoSteiner [16] and OAREST in Table 5. Instances with no overlaps are regarded as successes. The failure cases are due to: 1) Generalization error: For example, the R50 data with 10 obstacles occupy 90 points (50 pins + 40 obstacle corners) for each instance, exceeding the maximum number of 50 pins during training. This results in generalization error and could be improved by covering the 50-90 pins during training. 2) Dense obstacles between pins: For some extreme cases when obstacles are dense and the generated rectilinear edges frequently overlap with these obstacles, OAREST will stop updating the activation masking to keep the linearity of batch inference. It is common for one hard sample in a batch to harm the efficiency of the entire batch in machine learning. In our setting, we pay more attention to GPU parallelization for multiple instances.

In some cases, the RL framework can also generate redundant edges in the RES; these are removed in a post-processing step.

B.2 Baselines

GeoSteiner [16]. GeoSteiner is an efficient exact algorithm to solve RSMT problems. Based on the characteristics that an optimal RSMT can always be found by combining full Steiner trees only, it first enumerates all possible full Steiner trees and then forms an RSMT. However, the time complexity is exponential to the number of pins.

R-MST [17]. Rectilinear Minimum Spanning Tree (R-MST) is an approximation approach for RSMT. It can efficiently construct RSMT within $O(n \log n)$ time complexity and is proved [45] to have the length at most 1.5x that of RSMT.

BGA [18]. BGA employs heuristics to optimize the result. By computing an R-MST first, BGA then repeatedly replace bad edges with better ones to minimize the total length of the R-MST.

FLUTE [19]. FLUTE computes a look-up table in advance for the instances $\leq$9 pins, and thus it is an exact algorithm for these instances. For large instances with $>$9 pins, FLUTE breaks the net into small nets that can be handled by the look-up table. Within this algorithm, the authors introduce an accuracy parameter A, which allows users to control the trade-off between accuracy and runtime when generating RSMTs. $A = 3$ is the default accuracy level of FLUTE, where the runtime and error are moderate. Conversely, $A = 18$ represents a higher accuracy level, which invests more computational resources to further reduce the error in wirelength estimation.

REST [5]. REST is an RL-based framework that trains an actor-critic network on random data. The actor network is responsible for predicting the next rectilinear edge pair to connect while the critic network is utilized to rapidly predict the total wirelength of the tree. The generated rectilinear edge sequence (RES) finally forms an RSMT. In this method, the authors introduce 8 transformations ($T = 8$) that rotate the point set by 0, 90, 180, 270 degrees, with/without the x- and y- axes swapping, and select the best result. These transformations will not change the RSMT solution but bring promising improvement in wirelength. The time overhead of REST ($T = 8$) is approximately 8$\times$ that of REST ($T = 1$).

OARST [20]. OARST is an OARSMT algorithm, but it contains a sequential process, including generating the obstacle-avoiding spanning graph (OASG), the obstacle-avoiding spanning tree (OAST), the obstacle-avoiding rectilinear spanning tree (OARST), and finally obtains the obstacle-avoiding rectilinear Steiner minimal tree (OARSMT). We use its intermediate result of OARST as a strong baseline.

ObSteiner [21]. ObSteiner implements OARSMT by employing a geometric approach that decomposes the problem into constructing and concatenating full Steiner trees (FSTs) among complex obstacles, while enhancing computational efficiency through virtual terminal additions and pruning strategies.

B.3 Model Structure

The main structure is revised from [5], which contains an actor network and a critic network. Both of these networks take a set of points $\mathcal{P} = \{p_0, p_1, \cdots, p_{n-1}\}$ as the input and pass through an embedder and an encoder. The actor network has an additional decoder mechanism. During training, $\mathcal{P}$ only contains pins. For inference, $\mathcal{P}$ is a combination of pins and obstacle vertices. Detailed illustration is as follows:

Embedder. Given the set $\mathcal{P}$, denote its position matrix as $\mathbf{P} \in \mathbb{R}^{n\times 2}$. Before passing it into the encoder, they are processed by an embedder module to transform the raw input into a higher-dimensional space suitable for encoding. The embeddings are masked by $\mathbf{m}^{\text{input}}$[3]. Specifically, the embedder is defined as:

$$\text{Embedder}(\mathbf{P}) = \text{BatchNorm}(\text{Conv1D}(\mathbf{P}^\top))^\top \circ \mathbf{m}^{\text{input}}, \tag{15}$$

where Conv1D is a 1×1 convolution that projects the input from 2 to d_{emb} dimensions, and BatchNorm [46] applies batch normalization to stabilize the embeddings.

The embedder ensures that the input points are transformed into embeddings $\mathbf{E}_{\text{embed}} \in \mathbb{R}^{n\times d_{\text{emb}}}$ with a richer feature representation, which are then fed into the encoder.

Encoder. The encoder is a mapping $\text{Encoder} : \mathbb{R}^{n\times d_{\text{emb}}} \to \mathbb{R}^{n\times d_{\text{enc}}}$. Specifically, the Encoder is constructed using a multi-head attention mechanism [47]. The encoder operates with a stack of layers, where each layer is composed of two sublayers: a multi-head attention layer and a position-wise feedforward layer. These sublayers are connected through residual connections, followed by batch normalization to stabilize and accelerate the training process. Formally, given the input $\mathbf{X}$ to an encoder layer:

$$\begin{aligned}\mathbf{X}' &= \text{BatchNorm}(\text{MultiHeadAttention}(\mathbf{X}, \mathbf{X}, \mathbf{X}) + \mathbf{X}),\\ \mathbf{Y} &= \text{BatchNorm}(\text{FeedForward}(\mathbf{X}') + \mathbf{X}').\end{aligned} \tag{16}$$

[3]Note that the vectors in this section are instance-level for simplicity, different from the batch-level matrices in Sec. 3.2.

The multi-head attention mechanism computes attention as:

$$\text{Attention}(\mathbf{Q}, \mathbf{K}, \mathbf{V}) = \text{softmax}\left(\frac{\mathbf{Q}\mathbf{K}^\top}{\sqrt{d_k}}\right)\mathbf{V}, \tag{17}$$

where $\mathbf{Q}, \mathbf{K}, \mathbf{V}$ are the query, key, and value matrices derived from the input $\mathbf{X}$, and d_k is the dimensionality of the keys. Multiple attention heads are concatenated and linearly projected back to the original dimension.

The position-wise feedforward layer applies two linear transformations with a ReLU activation in between:

$$\text{FeedForward}(\mathbf{X}) = \text{ReLU}(\mathbf{X}\mathbf{W}_1 + \mathbf{b}_1)\mathbf{W}_2 + \mathbf{b}_2. \tag{18}$$

This encoder ensures that the representations are enriched with global contextual information while maintaining computational efficiency.

Forward Pass of Actor Network. The overall forward pass through the model begins with the embedder. The embeddings are then processed by the encoder, followed by a series of 1D convolutions to extract specific features:

$$\begin{aligned}
&\mathbf{E}_{\text{embed}} = \text{Embedder}(\mathbf{P}), \;\; \mathbf{E}_{\text{enc}} = \text{Encoder}(\mathbf{E}_{\text{embed}}),\\
&\mathbf{E}_{\text{r}} = \text{Conv1D}_r(\mathbf{E}_{\text{enc}}^\top)^\top, \;\; \mathbf{E}_{\text{x}} = \text{Conv1D}_x(\mathbf{E}_{\text{enc}}^\top)^\top, \;\; \mathbf{E}_{\text{y}} = \text{Conv1D}_y(\mathbf{E}_{\text{enc}}^\top)^\top,\\
&\mathbf{E}_{\text{xy}} = [\mathbf{E}_{\text{x}}, \mathbf{E}_{\text{y}}],
\end{aligned} \tag{19}$$

where Conv1D_r, Conv1D_x, and Conv1D_y are 1×1 convolution layers applied to the encoder output $\mathbf{E}_{\text{enc}}$, and $[\cdot, \cdot]$ represents concatenation along the feature dimension. This structured processing pipeline ensures that the model captures local and global information from the input points, preparing the features for subsequent decoding tasks.

Forward Pass of Critic Network. The critic network is designed to evaluate the quality of a solution by predicting the expected output length, providing a baseline for reinforcement learning. The forward pass of the critic network is as follows:

$$\begin{aligned}
&\mathbf{E}_{\text{embed}} = \text{CritEmbedder}(\mathbf{P}), \;\; \mathbf{E}_{\text{enc}} = \text{CritEncoder}(\mathbf{E}_{\text{embed}}),\\
&\mathbf{G} = \text{Glimpse}(\mathbf{E}_{\text{enc}}) = \text{softmax}(\tanh(\mathbf{E}_{\text{enc}})\mathbf{g}')^\top \mathbf{E}_{\text{enc}},\\
&\mathbf{o} = \text{MLP}(\mathbf{G}),
\end{aligned} \tag{20}$$

where CritEmbedder and CritEncoder respectively have the same structures of Embedder and Encoder with different learnable parameters. Glimpse computes a weighted sum of the encoded representations with $\mathbf{g}' \in \mathbb{R}^{d_{\text{enc}}}$. Finally, a multi-layer perception (MLP) is used that outputs the final predictions $\mathbf{o}$.

Decoder of Actor Network. The decoder of the actor network operates as a sequential decision-making process to generate rectilinear edges along with their associated probabilities. We show the whole process in Alg. 1, where the steps marked in blue means that they are executed only for inference phase. This decoder leverages pointer networks [48] with various masking strategies to compute logits. These logits are generated using encoded features and dynamically updated query vectors as inputs. At each step, the decoder selects indices based on computed logits, ensuring constraints such as unvisited points and obstacle avoidance are met. Additionally, the decoder employs activation masks to handle overlaps with obstacles, iteratively refining selections until a valid edge is identified. This mechanism helps the output rectilinear edge sequence and the cumulative log-probabilities adhere to the given spatial and logical constraints.

B.4 Training Strategy

Our training strategy consists of two phases. The first phase follows the methodology described in [5], while the second phase involves a quick multi-degree finetuning.

In the first phase, the model is sequentially trained from degree 3 to 50. After completing training at degree t, the parameters are used to initialize training at degree $t + 1$. Each degree-specific training involves 40,000 iterations with a batch size B that decreases as the degree increases. Specifically, B starts at 4096 for degree 3 and is progressively reduced to 2048, 1024, and 512 for degrees 10, 20, and

Algorithm 1 Actor Decoder

```
Input: Encoded features $\mathbf{E}_{\text{enc}}$, $\mathbf{E}_{\text{r}}$, $\mathbf{E}_{\text{xy}}$, obstacles $\mathcal{O}$.
Output: RES $r$ and cumulative log-probabilities $p$.
1: Initialize input mask $\mathbf{m}^{\text{input}}$, visited mask $\mathbf{m}^{\text{visited}}$, obstacle mask $\mathbf{m}^{\text{ob}}$, and activation masks $\mathbf{m}^{\text{act}}$.
2: Initialize the log-probabilities $p = 0$ of selecting a RES.
3: Define zero-initialized query vector $\mathbf{q}_0$.
4: Compute logits $\mathbf{s}_0 = \text{PointerStart}(\mathbf{E}_{\text{r}}, \mathbf{q}_0) \circ (\mathbf{m}^{\text{input}} \wedge \mathbf{m}^{\text{ob}})$.        Select the start point.
5: Sample starting index $v_0$ from $\mathbf{s}_0$. Denote $v^{(2)} = v_0$.
6: Update visited mask $\mathbf{m}^{\text{visited}}$.
7: for $j = 1$ to $n - 1$ do
8:     Compute the first query $\mathbf{q}_1$ based on $v^{(2)}$.
9:     Compute logits $\mathbf{s}^{(1)} = \text{Pointer1}(\mathbf{E}_{\text{r}}, \mathbf{q}_1) \circ (\mathbf{m}^{\text{input}} \wedge \mathbf{m}^{\text{visited}})$.        Select the unvisited point.
10:    Sample or determine first index $v^{(1)}$ from $\mathbf{s}^{(1)}$.
11:    Compute the second query $\mathbf{q}_2$ based on $v^{(1)}$.
12:    Compute logits $\mathbf{s}^{(2)} = \text{Pointer2}(\mathbf{E}_{\text{xy}}, \mathbf{q}_2) \circ (\mathbf{1} - \mathbf{m}^{\text{visited}})$.        Select the visited point.
13:    Sample or determine second index $v^{(2)}$ from $\mathbf{s}^{(2)}$.
14:    Decode indices $x, y$ from $v^{(1)}, v^{(2)}$.
15:    while $(x, y)$ overlaps obstacles $\mathcal{O}$ do
16:        Update activation masks $\mathbf{m}^{\text{act}}$;
17:        Compute logits $\mathbf{s}^{(1)} = \text{Pointer1}(\mathbf{E}_{\text{r}}, \mathbf{q}_1) \circ (\mathbf{m}^{\text{input}} \wedge \mathbf{m}^{\text{visited}} \wedge \mathbf{m}^{\text{act}})$.        Select the new unvisited point.
18:        Sample or determine first index $v^{(1)}$ from $\mathbf{s}^{(1)}$.
19:        Compute logits $\mathbf{s}^{(2)} = \text{Pointer2}(\mathbf{E}_{\text{xy}}, \mathbf{q}_2) \circ (\mathbf{1} - \mathbf{m}^{\text{visited}})$.        Select the new visited point.
20:        Sample or determine second index $v^{(2)}$ from $\mathbf{s}^{(2)}$.
21:        Decode indices $x, y$ from $v^{(1)}, v^{(2)}$.
22:    end while
23:    Add the rectilinear edge $(x, y)$ to RES $r$.
24:    Compute $\log p(v^{(1)}), \log p(v^{(2)})$ from $\mathbf{s}^{(1)}, \mathbf{s}^{(2)}$ and add to $p$.
25:    Update visited mask $\mathbf{m}^{\text{visited}}$.
26: end for
```

40, respectively. The Adam optimizer [49] is employed with an initial learning rate of 2.5×10^{-4}, which decays by a factor of 0.96 after each degree's training.

In the second phase, we leverage a dynamic masking strategy to jointly train the model across a range of degrees, from n_1 to n_2. The Adam optimizer is again utilized, this time with a learning rate of 5×10^{-5}. The total number of iterations in this phase is limited to the number of iterations required for training a single degree in the first phase. Specifically, we conduct training for the degree ranges (n_1, n_2) as follows: $(3, 10)$, $(10, 20)$, $(20, 30)$, $(30, 40)$, $(40, 50)$, and $(3, 50)$.

B.5 Inference Strategy

For the RSMT problems, we use OAREST (3-10) to test R5 and R10, OAREST (10-20) to test R15 and R20, and so forth. For each group of instances, a batch size of $100\,\text{k}/$*degree* is used for parallel inference. To further enhance the performance, we use 8 transformations proposed by [5] that rotate the point set by 0, 90, 180, 270 degrees, with/without the x- and y- axises swapping, and select the best result. These transformations will not change the RSMT solution but bring promising improvement in wirelength.

For the OARSMT problems, we use OAREST (40-50) for all groups of instances due to large occupations of obstacles. To demonstrate the efficiency of GPUs, we use the full batch size, i.e., $10\,\text{k}$, for parallel inference. To keep the linearity of inference, the model only inspects the obstacles once for the 'while' in Alg. 1. Here, 8 transformations are also used.

B.6 Visualization

In this section, we present the visualized results of OARSMTs with 5-50 pins and 0/5/10 obstacles. When no obstacles are present, the OARSMT results are the same as the vanilla RSMTs. As shown in Fig. 8-17, each line represents three pairs of instances with the same number of pins, including the pair without obstacles (left), with 5 obstacles (middle), and with 10 obstacles (right). Within each pair, the left means the result obtained by the exact RSMT algorithm GeoSteiner [16] and the right represents the result obtained by OAREST.

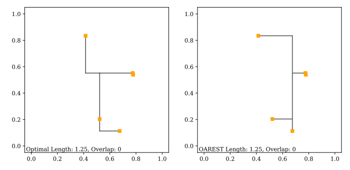
Optimal Length: 1.25, Overlap: 0
OAREST Length: 1.25, Overlap: 0
(a) 5 pins.

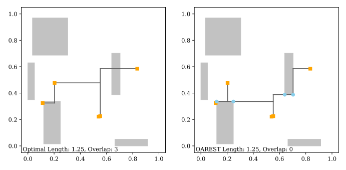
Optimal Length: 1.25, Overlap: 3
OAREST Length: 1.25, Overlap: 0
(b) 5 pins & 5 obstacles.

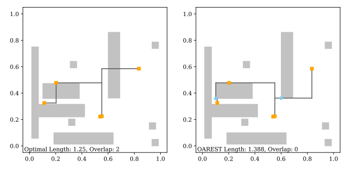
Optimal Length: 1.25, Overlap: 2
OAREST Length: 1.388, Overlap: 0
(c) 5 pins & 10 obstacles.

Figure 8: OARSMT with 5 pins and 0/5/10 obstacles.

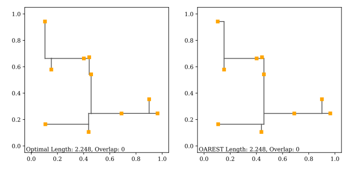
Optimal Length: 2.248, Overlap: 0
OAREST Length: 2.248, Overlap: 0
(a) 10 pins.

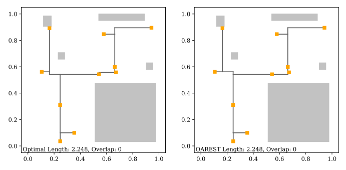
Optimal Length: 2.248, Overlap: 0
OAREST Length: 2.248, Overlap: 0
(b) 10 pins & 5 obstacles.

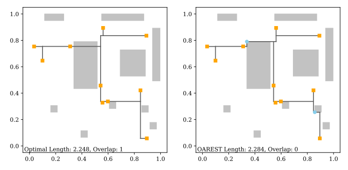
Optimal Length: 2.248, Overlap: 1
OAREST Length: 2.284, Overlap: 0
(c) 10 pins & 10 obstacles.

Figure 9: OARSMT with 10 pins and 0/5/10 obstacles.

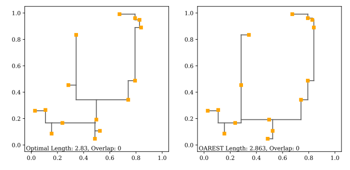
Optimal Length: 2.83, Overlap: 0
OAREST Length: 2.863, Overlap: 0
(a) 15 pins.

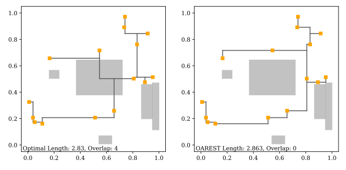
Optimal Length: 2.83, Overlap: 4
OAREST Length: 2.863, Overlap: 0
(b) 15 pins & 5 obstacles.

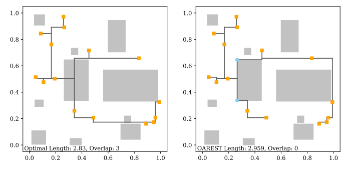
Optimal Length: 2.83, Overlap: 3
OAREST Length: 2.959, Overlap: 0
(c) 15 pins & 10 obstacles.

Figure 10: OARSMT with 15 pins and 0/5/10 obstacles.

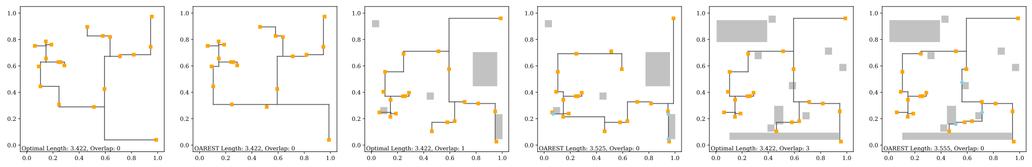

(a) 20 pins. (b) 20 pins & 5 obstacles. (c) 20 pins & 10 obstacles.

Figure 11: OARSMT with 20 pins and 0/5/10 obstacles.

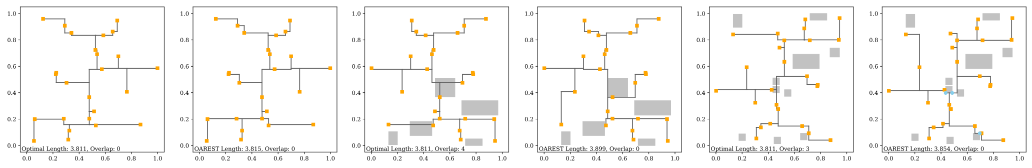

(a) 25 pins. (b) 25 pins & 5 obstacles. (c) 25 pins & 10 obstacles.

Figure 12: OARSMT with 25 pins and 0/5/10 obstacles.

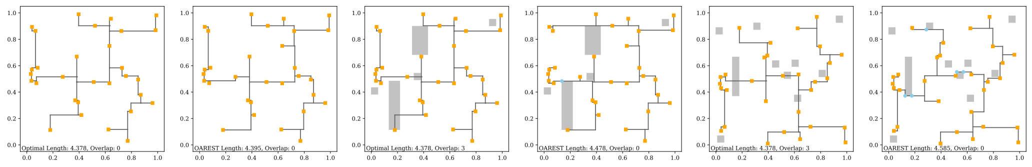

(a) 30 pins. (b) 30 pins & 5 obstacles. (c) 30 pins & 10 obstacles.

Figure 13: OARSMT with 30 pins and 0/5/10 obstacles.

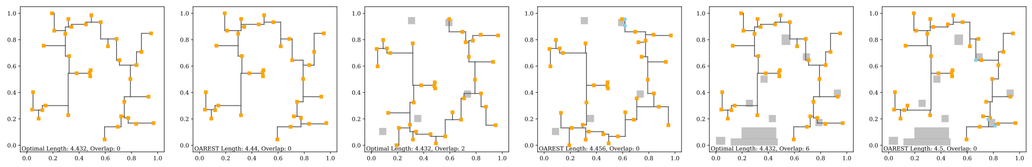

(a) 35 pins. (b) 35 pins & 5 obstacles. (c) 35 pins & 10 obstacles.

Figure 14: OARSMT with 35 pins and 0/5/10 obstacles.

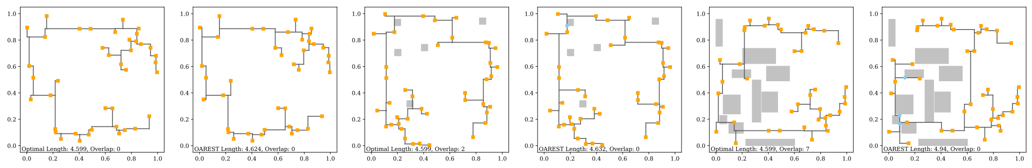

(a) 40 pins. (b) 40 pins & 5 obstacles. (c) 40 pins & 10 obstacles.

Figure 15: OARSMT with 40 pins and 0/5/10 obstacles.

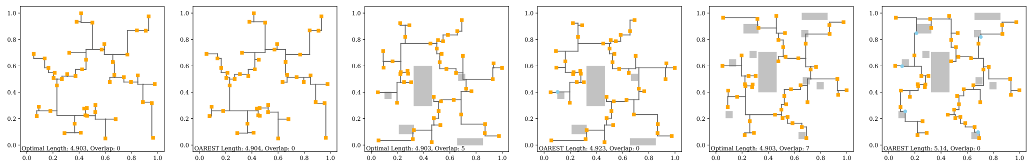

(a) 45 pins. (b) 45 pins & 5 obstacles. (c) 45 pins & 10 obstacles.

Figure 16: OARSMT with 45 pins and 0/5/10 obstacles.

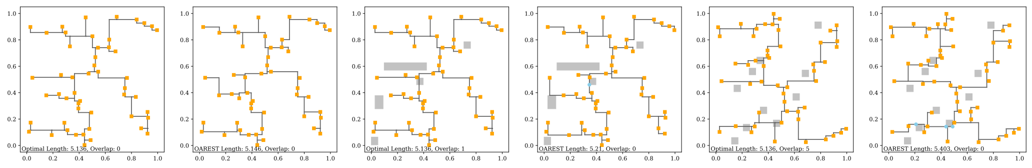

(a) 50 pins. (b) 50 pins & 5 obstacles. (c) 50 pins & 10 obstacles.

Figure 17: OARSMT with 50 pins and 0/5/10 obstacles.